DOI: 10.1534/genetics.107.081356

Multiple Functions and Dynamic Activation of MPK-1 Extracellular Signal-Regulated Kinase Signaling in *Caenorhabditis elegans* Germline Development

Min-Ho Lee,*[,1,2] Mitsue Ohmachi,*[,1] Swathi Arur,* Sudhir Nayak,*[,3] Ross Francis,*[,4] Diane Church,[†] Eric Lambie[†] and Tim Schedl*[,5]

**Department of Genetics, Washington University School of Medicine, St. Louis, Missouri 63110 and [†]Department of Biological Sciences, Dartmouth College, Hanover, New Hampshire 03755*

Manuscript received August 30, 2007
Accepted for publication September 20, 2007

ABSTRACT

The raison d'etre of the germline is to produce oocytes and sperm that pass genetic material and cytoplasmic constituents to the next generation. To achieve this goal, many developmental processes must be executed and coordinated. ERK, the terminal MAP kinase of a number of signaling pathways, controls many aspects of development. Here we present a comprehensive analysis of MPK-1 ERK in *Caenorhabditis elegans* germline development. MPK-1 functions in four developmental switches: progression through pachytene, oocyte meiotic maturation/ovulation, male germ cell fate specification, and a nonessential function of promoting the proliferative fate. MPK-1 also regulates multiple aspects of cell biology during oogenesis, including membrane organization and morphogenesis: organization of pachytene cells on the surface of the gonadal tube, oocyte organization and differentiation, oocyte growth control, and oocyte nuclear migration. MPK-1 activation is temporally/spatially dynamic and most processes appear to be controlled through sustained activation. MPK-1 thus may act not only in the control of individual processes but also in the coordination of contemporaneous processes and the integration of sequential processes. Knowledge of the dynamic activation and diverse functions of MPK-1 provides the foundation for identification of upstream signaling cascades responsible for region-specific activation and the downstream substrates that mediate the various processes.

IN the generation of oocytes and sperm, perhaps the most complex cells in animals, the germline lineage undergoes a multifaceted developmental process that begins in embryogenesis and continues into adulthood. While the details of the steps can differ between species due to differences in reproductive biology, a core set of events occurs in animals: germ cell fate specification, incorporation into the gonad, sexual fate specification, proliferative expansion, and gamete production. Two interconnected differentiation programs define gamete production: (1) meiosis where chromosomes pair, recombine, and then segregate to give a reassorted haploid content and (2) gametogenesis where biosynthetic and morphogenetic processes generate the large nutrient and developmental information-rich oocyte and the small motile sperm. In aggregate, these processes are essential to pass genetic material from generation to generation and to form the totipotent zygote necessary for the development of a new individual. Disruption of germline development can lead to sterility, germline tumors, and birth defects. Thus an important goal is to define the pathways and gene products that control and execute the various steps of germline development.

The MAP kinase extracellular signal-regulated kinase (ERK) functions in many aspects of animal development and homeostasis (Marshall 1995; Rubin *et al.* 1997; Schlessinger 2000; Sundaram 2006). ERK is the terminal regulator of signaling cascades such as canonical receptor tyrosine kinase signaling, which contains core members, including the RAS GTPase, the MAP kinase kinase kinase Raf, and the MAP kinase kinase MEK that activates ERK. In *Caenorhabditis elegans*, the ERK ortholog MPK-1 (Lackner *et al.* 1994; Wu and Han 1994), as well as orthologs of the upstream cascade members LET-60 Ras, KSR-1 and -2 KSR, LIN-45 Raf, and MEK-2 MEK, function in vulval cell fate specification, cell migration/guidance, defense against bacterial infection, and other processes (reviewed in Moghal and Sternberg 2003; Sundaram 2006). Ras–ERK signaling is also important for *C. elegans* germline development as

[1]These authors contributed equally to this work.

[2]*Present address:* Department of Biological Sciences, SUNY, Albany, NY 12222.

[3]*Present address:* Department of Biology, The College of New Jersey, P.O. 7718, Ewing, NJ 08628-0718.

[4]Exelixis, P.O. Box 511, South San Francisco, CA 94083-051.

[5]*Corresponding author:* Department of Genetics, Washington University School of Medicine, Campus Box 8232, 4566 Scott Ave., St. Louis, MO 63110. E-mail: ts@genetics.wustl.edu

loss-of-function (lf), but not null, alleles of *let-60*, *mek-2*, and *mpk-1*, as well as null alleles of *ksr-2*, result in germ cells arrested in pachytene (Church *et al.* 1995; Ohmachi *et al.* 2002). The pachytene-arrest phenotype, which is observed in both hermaphrodites and males, was interpreted as an essential function of these genes in the transition from pachytene to diplotene (pachytene exit; Church *et al.* 1995). In vertebrates, ERK functions in meiotic maturation of full-grown oocytes and/or arrest at metaphase of meiosis II prior to fertilization (reviewed in Fan and Sun 2004; Liang *et al.* 2007); however, little is known about ERK function in the many earlier steps of germline development.

Since the initial report of Church *et al.* (1995), new mutations in a number of the core pathway genes have been identified: null alleles of *mpk-1* and *lin-45*, a temperature-sensitive (ts) *mpk-1* lf allele (*ga111*) that allows examination of MPK-1 function in late steps of germline development, and a ts *let-60* gain-of-function (gf) allele (*ga89*) that permits examination of the effect of increased MPK-1 activation (Eisenmann and Kim 1997; Lackner and Kim 1998; Hsu *et al.* 2002). Molecular markers that allow stages of germline development to be more fully defined and the sex of immature germ cells to be determined have also been identified. An initial description of the pattern of MPK-1 activation (the MEK-2 MEK diphosphorylated form of MPK-1, dpMPK-1) in the hermaphrodite germline has been presented, but not analyzed in the context of core pathway mutant backgrounds (Miller *et al.* 2001; Page *et al.* 2001). MPK-1 activation was found to correlate with oocyte meiotic maturation, consistent with ERK playing a role in the process as it does in other organisms, but experiments have not addressed the importance of *mpk-1* function in the maturation process. Here we build on previous studies using the new mutations and molecular markers in a comprehensive analysis of MPK-1 function and activation in hermaphrodite and male germlines. We found that MPK-1 has diverse germline functions, acting in four developmental switches and in four aspects of cell biology during oogenesis. MPK-1 activation is temporally/spatially dynamic compared to relatively constant levels of total MPK-1, and most processes appear to be controlled by sustained activation. Below we briefly review aspects of *C. elegans* germline development relevant to this study.

C. elegans is an excellent system for analysis of germline development due to facile genetics and favorable anatomy where most of the processes are ongoing in the adult and can be studied in real time, as live animals are transparent, and with fixed specimens (reviewed in Hubbard and Greenstein 2000). The adult hermaphrodite has two U-shaped gonads while the male has a single U-shaped gonad (Figure 1, B and D, linear projection diagrams of single gonads). The hermaphrodite is considered to be female in somatic tissues with the germline undergoing male development (spermatogenesis) transiently in the third larval (L3) and L4 stages and female development (oogenesis) from L4 throughout adulthood. The male has a male soma and undergoes spermatogenesis from L3 through adulthood. The germline sex determination pathway controls the decision between female and male germline development (reviewed in Ellis and Schedl 2006). The U-shaped gonads have germ cells arranged in a distal-to-proximal polarity with respect to the somatic distal tip cell at the distal end in both sexes and the proximal spermatheca/uterus in the hermaphrodite or the vas deferens in the male. Germ cells progress proximally in an assembly-line-like fashion with the germline divided into regions based on chromosome and cellular morphology. At the distal end, germ cells proliferate (mitotic zone) under control of GLP-1 Notch signaling (reviewed in Hansen and Schedl 2006; Kimble and Crittenden 2006); in wild type, this region contains ~220 cells and extends ~20 cell diameters in length proximally from the distal tip. At the proximal end of the mitotic region, germ cells switch to meiotic prophase where they are first in leptotene/zygotene (transition zone, or TZ) and then progress through an extended pachytene region that is then followed by diplotene and diakinesis where overt gamete formation occurs. Meiotic prophase of oogenesis lasts 54–60 hr while meiotic prophase for spermatogenesis in males lasts 20–24 hr (Jaramillo-Lambert *et al.* 2007). Much of the germline is a syncytium; plasma membranes do not fully surround each nucleus and a "window" connects each to a common cytoplasm. By convention, each nucleus, surrounding cytoplasm, and membranes are referred to as a germ cell. From the mitotic region through the end of pachytene, germ cells are arranged on the surface of the gonadal tube with an interior cell/nucleus-free cytoplasmic region called the rachis or core. Consistent with the longer time of meiotic prophase, oogenesis has complexities that are lacking in spermatogenesis. In oogenesis, the majority of pachytene cells appear to function as nurse cells, undergoing apoptosis after providing RNAs and proteins to the rachis (Gibert *et al.* 1984; Gumienny *et al.* 1999; Wolke *et al.* 2007). As germ cells progress from pachytene to diplotene in the loop region, oocyte differentiation begins; a single-file row of growing oocytes is on the external surface while the rachis that is supplying cytoplasm to growing oocytes is found on the internal surface (external/internal refer to the loop of the U-shaped gonad). The proximal approximately five oocytes (-1 through -5) are in diakinesis and are apparently fully cellularized as they are no longer connected to the rachis (Maddox *et al.* 2005). In the adult hermaphrodite, sperm are stored in the spermatheca, the site of fertilization. In the single-file assembly line, the most proximal oocyte, the -1 oocyte, undergoes meiotic maturation (nuclear envelope breakdown, progression to metaphase of meiosis I, and cortical rearrangement), is ovulated into the spermatheca and fertilized (McCarter

et al. 1999). The -2 oocyte then moves into the -1 position where it will undergo maturation/ovulation ~23 min later. In hermaphrodites with sperm, the signal that triggers maturation/ovulation is constitutive: the major sperm protein (MSP) secreted from sperm (McCarter *et al.* 1999; Miller *et al.* 2001; Kosinski *et al.* 2005). By contrast, in animals without sperm (sex determination mutant females, adult hermaphrodites that have exhausted their self-sperm), oocytes form but are arrested in diakinesis.

MATERIALS AND METHODS

Strains: The following mutations were used in this study: LGI, *mek-2(h294)*, *mek-2(q425)*, *mek-2(q484)*, *mek-2(n2678)*, *mek-2(oz221)*, *mek-2(dx51)*, *mek-2(n1859)*, *rrf-1(pk1417)*, *glp-4(bn2)*; LGII, *tra-2(e1095)*; LGIII, *mpk-1(ga117)*, *mpk-1(ga111ts)*, *mpk-1(oz140)*, *unc-32(e189)*, *glp-1(bn18ts)*, *mrt-2(e2663)*; LGIV, *unc-5(e53)*, *let-60(ga89gf)*, *let-60(n1046)*, *lin-45(oz201)*, *lin-45(dx19)*, *lin-45(dx89)*, *fem-3(e1996)*, *spo-11(ok79)*, *him-8(e1489)*; and LGV, *fog-2(oz40)*, *mre-11(ok179)*.

Nematode strains and culture: Standard procedures for culture and genetic manipulation of *C. elegans* strains were followed with growth at 20° unless otherwise noted (Sulston and Hodgkin 1988). Descriptions of genes, alleles, and phenotypes related to this study are in Church *et al.* (1995), Eisenmann and Kim (1997), Lackner and Kim (1998), and Hsu *et al.* (2002) or are cited in the text as genes, alleles, and phenotypes are mentioned.

Antibodies and reagents: The following antibodies were used in this study: anti-MAPKYT antibody (Sigma, St. Louis) used at 1:400; anti-SYN-4/PTC-1 antibodies (kind gifts from Michael Glotzer and Patty Kuwabara) used at 1:400 and 1:50, respectively (these two antibodies were mixed together for visualizing membrane morphology); anti-AIR-2 antibody (kind gift from Jill Schumacher) used at 1:50 dilution (to detect the chromosomes undergoing maturation/ovulation); anti-REC-8 (kind gift from Josef Loidl) used at 1:100; anti-HIM-3 (kind gift from Monique Zetka) used at 1:100 as described (Hansen *et al.* 2004); anti-DAZ-1 (kind gift from Masayuki Yamamoto) used at 1:50; anti-CEP-1 (kind gift from Anton Gartner) used at 1:50; anti-CGH-1 (a kind gift from David Greenstein) used at 1:400; and anti-GLD-1 used at 1:200. Anti-NOP-1 (Encor Biotech) was used at 1:200. Rhodamine–phalloidin was used at 1:100 to visualize actin cytoskeleton. Secondary antibodies were donkey anti-mouse Alexa 594, goat anti-rabbit Alexa 488, goat anti-rabbit Alexa 594, goat anti-rat Alexa 488, and donkey anti-goat Alexa 594, obtained from Molecular Probes (Eugene, OR).

Anti-ERK antibody SC94 (Santa Cruz), while giving a relatively specific MPK-1 pattern on Western blots (supplemental Figure 1 at http://www.genetics.org/supplemental/), showed significant germline cytological staining in *mpk-1(ga117)* null gonads indicative of nonspecific reactivity. The peptide used as the immunogen for SC94, corresponding to residues 305–327 of human ERK1, contains sequences in the N-terminal half that may cross-react with *C. elegans* MAP kinases W06F12.1 (*lit-1*) and F42G8.4 (*pmk-3*). Therefore, a peptide (KRITVEEALAPHY) corresponding to the N-terminal portion of the immunogen was used to subtract antibodies in SC94 that might cross-react with other *C. elegans* MAP kinases. The SC94 antiserum was passed over a KRITVEEALAPHY-linked column and the flow through, designated SC94-C, was collected. SC94-C, used at 1:25 dilution, shows no germline staining in *mpk-1(ga117)* germlines although it displays some cross-reactivity in the somatic gonad (supplemental Figure 2B). We also tested anti-ERK2 from Zymed; however, this antibody detected a strong signal in *mpk-1(ga117)* germlines and was not used further.

Western analysis: L4 hermaphrodites of given genotypes were hand picked, grown for 48 hr or the indicated time at the indicated temperature, and then harvested for Western analysis as previously described (Jones *et al.* 1996). The extracts were resolved on 10% SDS–PAGE (acrylamide/*bis*-acrylamide is 100/1), transferred to PVDF membrane, and probed with SC94 (Santa Cruz) at 1:2000 dilution, MAPKYT at 1:10,000 dilution, or MH16 (antiparamyosin antibody) at 1:15,000 dilution. The Western blots were developed using SuperSignal West Pico chemiluminescent substrate from Peirce on Kodak BioMax MS film.

Antibody staining: For antibody staining, dissected gonads (Jones *et al.* 1996) of the indicated genotype were fixed in 3% formaldehyde with 100 mm K_2HPO_4 (pH 7.2) for 1 hr at room temperature (or 10 min for DAZ-1, REC-8, and HIM-3) and postfixed with 100% methanol (−20°) for 5 min (Francis *et al.* 1995). Fixed gonads, in batches, were blocked with 30% normal goat serum (NGS), or 1% BSA for CEP-1, in 1× PBS plus 0.1% Tween-20 (termed blocking buffer) for 1 hr at room temperature before incubation with the desired primary antibody. In all cases, the primary and secondary antibody incubations were at indicated dilutions in blocking buffer followed by washes with blocking buffer (Jones *et al.* 1996).

For dpMPK-1 staining, gonads were in fixative within 5 min of beginning the dissection as longer dissection times can result in reduced dpMPK-1 staining. To verify that the dpMPK-1 staining pattern was not altered through the dissection procedure, wild-type adult hermaphrodite whole-mount freeze-crack preparations were generated (Jones *et al.* 1996) and found to show essentially the same staining pattern as dissected gonads (data not shown). When dpMPK-1 levels were to be compared to genotypes that differed in morphology, they were dissected, fixed, blocked, stained, and washed together in batches and mounted on the same slide, and images were captured at the same settings and processed identically. When genotypes had similar morphology, given genotypes were differentially stained for identification (*e.g.*, only one stained for SYN-4/PTC-1) and then combined for dpMPK-1 staining and subsequent steps. In many cases, *mpk-1(ga117)* gonads were included to provide a no-signal baseline.

RNA *in situ* hybridization: Dissected gonads were fixed in 0.25% glutaraldehyde/3% formaldehyde, 100 mm K_2HPO_4, pH 7.2 (Jones *et al.* 1996). Both *rme-2* sense and antisense probes were synthesized using primer extension and digoxigenin-11-dUTP. The control *rme-2* sense probe gave little or no signal (data not shown). Images were captured with a Zeiss Axioplan 2 microscope equipped with a SPOT digital CCD camera (Diagnostic Instruments).

Image capture and processing: Fluorescent images were captured with a Zeiss Axioskop microscope equipped with Hamamatsu digital CCD camera (Hamamatsu Photonics). All images were taken as a montage at ×63 and processed identically with Adobe Photoshop v7. All images for a given antibody staining were taken with identical exposures, unless otherwise indicated.

Measurement of oocyte size and dpMPK-1 staining intensity: Wild-type and *mpk-1(ga111)* hermaphrodites were synchronized at mid-L4, grown at 20° for 16 hr, shifted to 25° for 8 hr, and stained with anti-SYN-4/PTC-1 antibodies. To measure the surface area of oocytes, we imported the anti-SYN-4/PTC-1-stained images (as tiff files) into the public domain National Institutes of Health Image program (http://rsb.info.nih.gov/nih-image/), traced the membrane surface of each oocyte at a given position along the SYN-4/PTC-1

staining pattern with an "area tool," and the measured pixel number represented as a bar graph.

For dpMPK-1 staining intensity, we synchronized wild-type and *let-60(ga89gf)* hermaphrodites and dissected the germlines 24 hr after mid-L4 stage at 20° and stained for dpMPK-1. To measure the intensity of dpMPK-1 staining, we imported the dpMPK-1 images (as tiff files) into NIH Image J. For pachytene intensity, a line was drawn to mark the distal and proximal ends of pachytene, and pixel intensity was graphed relative to distal–proximal cell position in pachytene. For oocyte intensity, a line was drawn around each oocyte with the area tool and the pixel intensity was measured. This was then divided by the area of each oocyte to normalize for the size of the oocyte, and the measure was represented as a bar graph to depict the signal intensity in the oocytes at each individual position.

For measuring dpMPK-1 accumulation variability between sibling oocytes in a given germline, we costained with anti-CGH-1 (a uniform cytoplasmic marker) to remove gonads that contain damaged oocytes with low/absent CGH-1 from the analysis. The dpMPK-1 intensity was assigned by increasing the gain in Adobe Photoshop v7 for each germline until the dpMPK-1 signal in at least one oocyte was saturated. This oocyte was assigned a ++++ value. Oocytes with a slightly lower strength (to ++++) were assigned +++ and so on. An oocyte that showed no signal at all, such as a maturing oocyte, was assigned zero.

Time-lapse video microscopy: To monitor maturation/ovulation, time-lapse video microscopy was used as described (McCarter *et al.* 1999).

RNA interference: The *mpk-1* RNA interference (RNAi) clone was obtained from Open Biosystems. Before analysis, the clone was sequenced to verify its identity. HT115(DE3) strain with the *mpk-1* RNAi clone was thawed from −80° storage and inoculated onto plates containing LB agar with 100 μg/ml ampicillin and 10 μg/ml tetracycline and grown overnight at 37°. Two to four colonies were inoculated into 2 ml LB with 100 μg/ml ampicillin and 10 μg/ml tetracycline and grown overnight at 37° rotator. The next day the culture was diluted 1:100 into LB with 100 μg/ml ampicillin and 10 μg/ml tetracycline and grown for 6 hr at 37°. RNAi bacteria were then seeded onto plates containing lactose (0.2%) and ampicillin (100 μg/ml) and incubated at room temperature for 3 days to grow bacteria and induce double-strand RNA. We transferred three to five gravid adults per plate for incubation at 20° (this plate was marked day 0). The gravid adults were transferred to new plates the following day (day 1). F_1 progeny were picked (from the day 0 and the day 1 plates) as L4 larvae (on fresh *mpk-1* RNAi plates) and scored 24 hr later or as indicated.

RESULTS

Spatial pattern of total and dpMPK-1 in the wild-type adult hermaphrodite germline: MPK-1 function is likely controlled largely through activation by signaling pathways but could also be regulated by limiting the amount of total MPK-1 accumulation. To distinguish between these possibilities, we employed the monoclonal antibody MAPKYT (Sigma; Miller *et al.* 2001; Page *et al.* 2001; Ohmachi *et al.* 2002) to detect the diphosphorylated activated form of MPK-1 (dpMPK-1), while to detect total MPK-1 we used a fraction of the SC94 antibody (Santa Cruz) that was affinity purified to show low cytological cross-reactivity in *mpk-1(ga117)* null germlines (see materials and methods and supplemental data at http://www.genetics.org/supplemental/ for further antibody characterization). In wild-type hermaphrodites 24 hr post mid-L4, total MPK-1 is found throughout the germline, with slightly lower levels in the distal-most end and slightly higher levels in the proximal region (Figure 1A; supplemental Figure 2A). Total MPK-1 is primarily cytoplasmic except in late-stage oocytes where there is nuclear enrichment. Consistent with previous studies, we find that dpMPK-1 is undetectable in the mitotic and transition zone regions, peaks in the proximal part of pachytene, becomes low but detectable in the loop region, and peaks again in diakinesis oocytes in the proximal gonad (Figures 1A and 2A; Miller *et al.* 2001; Page *et al.* 2001). Thus MPK-1 activation appears to be controlled primarily through signaling-pathway-mediated phosphorylation/dephosphorylation, rather than through regulation of MPK-1 accumulation, although we have not addressed whether other core members of the cascade are regulated at the level of protein accumulation.

As a first step in understanding the relationship between MPK-1 function and activation, we visually determined the cellular position of dpMPK-1 accumulation along the distal–proximal length of the germline in cell diameters from the distal tip (Figure 3B). In wild-type hermaphrodites 24 hr post mid-L4, the pachytene region is 37 (±2) cell diameters in length. dpMPK-1 is first detected almost midway through pachytene at 45 (±3) cell diameters from the distal tip, or ~46% of the length of pachytene, with the rise occurring in 3 (±1) cell diameters, plateaus for 10 (±1) cell diameters, and then falls for 5 (±1) cell diameters, concluding 2 (±1) cell diameters prior to the end of pachytene. dpMPK-1 is observed equivalently in the cytoplasm and nuclei of surface proximal pachytene cells and in the corresponding cytoplasm of the interior rachis. The valley of low dpMPK-1 in the loop region from very late pachytene through early diakinesis is 7 (±1) cell diameters and is followed by high, but dynamically variable, levels in late-stage diakinesis oocytes (see below).

MPK-1 is necessary for the progression from distal to proximal pachytene: Previous analysis of nuclear morphology in lf *let-60* RAS, *mek-2* MEK, and *mpk-1* mutants (Church *et al.* 1995) and null *ksr-2* KSR mutants (Ohmachi *et al.* 2002) indicated that, in the distal hermaphrodite gonad, germ cells proliferate, enter meiotic prophase, and progress to pachytene normally but fail to advance to diplotene and diakinesis, resulting in pachytene-arrested nuclei in the proximal gonad. Similarly, we find that germ cells are arrested in pachytene in null *mpk-1* and *lin-45* RAF mutants and strong lf *mek-2* mutants. dpMPK-1 fails to accumulate in *mpk-1* null, strong lf *mek-2* mutants, and young adult *lin-45* mutants (Table 1; Figure 3D; supplemental Figures 1 and 2C at http://www.genetics.org/supplemental/). *mpk-1(ga111)* is a ts lf mutant (Lackner and Kim 1998). At the restrictive temperature, there is a strong but incompletely penetrant pachytene-arrest phenotype

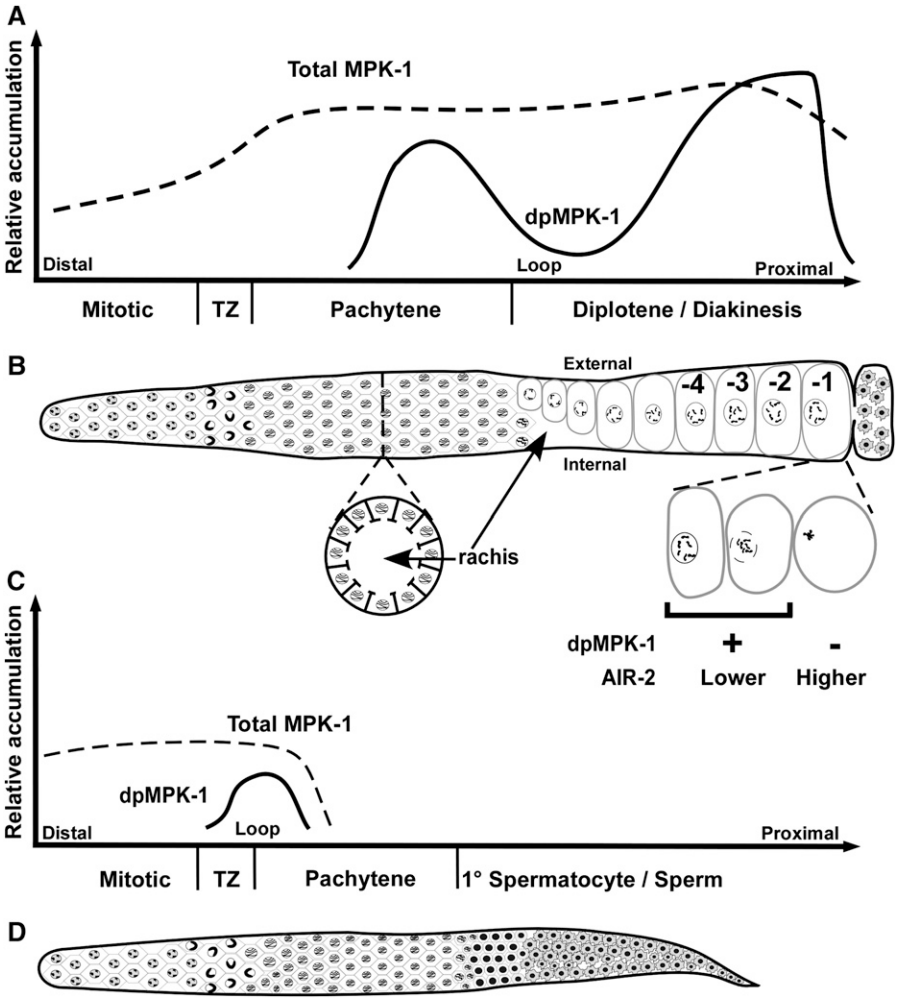

Figure 1.—Summary of MPK-1 activation in relation to adult hermaphrodite and male germline development. Schematics of total MPK-1 and dpMPK-1 accumulation relative to the corresponding regions of adult hermaphrodite (A and B) and male (C and D) germline development. In all panels, distal is to the left and proximal is to the right. (A) Total MPK-1 levels (dashed line) in oogenesis are derived from supplemental Figure 2A (at http://www.genetics.org/supplemental/) and dpMPK-1 levels (solid line) are from Figure 2A, Figure 3, A and B, Figure 4, and supplemental Figures 4A, 7, and 8A. (B) Corresponding linear projection diagram of the adult hermaphrodite germline. Surface view distal to the loop shows germ cells organized in a hexagonal pattern from the mitotic region, the TZ through the end of pachytene. Below is a cross section in mid-pachytene showing cells arranged on the surface of the gonadal tube, the interior cell/nucleus-free cytoplasm called the rachis, and connecting passages that allow newly synthesized materials in germ cells to be deposited into the rachis. Proximal to the loop is an internal view showing growing oocytes on the external side, relative to the U-shaped gonad, and the rachis on the internal side, followed by late-stage oocytes that are numbered consecutively from the most proximal -1 oocyte, adjacent to the spermatheca. Below, the -1 oocyte is shown as it undergoes maturation, which includes nuclear envelope breakdown, congression of bivalents to the meiosis I metaphase plate, and cortical rearrangement; dpMPK-1 falls during maturation in a pattern that is opposite that of chromosomal AIR-2 staining. Neither the somatic distal tip cell nor the somatic gonadal sheath cells that surround the proximal two-thirds of the germline are shown. (C) Total MPK-1 in male spermatogenesis is derived from supplemental Figure 13 while dpMPK-1 is from Figure 7. (D) Corresponding linear projection diagram of the adult male germline, with a surface view of hexagonally packed germ cells from the mitotic region through the end of pachytene followed by primary (1°) spermatocytes and then sperm. See text for details.

(Table 2) and dpMPK-1 levels are very low in the gonad distal to the loop while variably patchy accumulation is observed in the proximal gonad (data not shown).

The rise in dpMPK-1 levels almost midway through pachytene suggests that active MPK-1 may promote progression through pachytene, possibly functioning to switch germ cells from a distal pachytene subtype to a proximal pachytene subtype. This is analogous to other systems, where in certain contexts activation of ERK orthologs can function in developmental switches to specify cell type (Rubin *et al.* 1997; Sundaram 2006). However, previously the pachytene-arrest phenotype in *let-60*, *mek-2*, and *mpk-1* mutants was interpreted as MPK-1 promoting the transition from pachytene to diplotene (termed pachytene exit; Church *et al.* 1995), with the implication that mutant germ cells are arrested at the end of pachytene just prior to diplotene. To distinguish between a role for MPK-1 in promoting pachytene progression *vs.* the transition from pachytene to diplotene, we used antibody markers to assess the stage within pachytene where germ cells are arrested in *mpk-1* null mutants. Steady-state levels of the RNA-binding protein DAZ-1 are high in the mitotic and transition zone and fall midway through pachytene in wild-type germlines (Maruyama *et al.* 2005). Costaining reveals that DAZ-1 and dpMPK-1 have reciprocal patterns, where the fall of DAZ-1 terminates at 52 (±3) cell diameters (~67% the length of pachytene), with a region of staining overlap of ~7 cell diameters (Figure 3, A and B). In *mpk-1* null germlines, DAZ-1 levels remain elevated throughout the extended pachytene region, indicating that the arrested pachytene cells have distal/mid-pachytene character rather than proximal/late pachytene character (Figure 3D). In wild type, levels of the RNA-binding protein GLD-1 are high from the mitotic/transition zone boundary through distal pachytene and begin falling about two-thirds of the way through the pachytene region (Jones *et al.* 1996). As GLD-1 levels fall, translation of

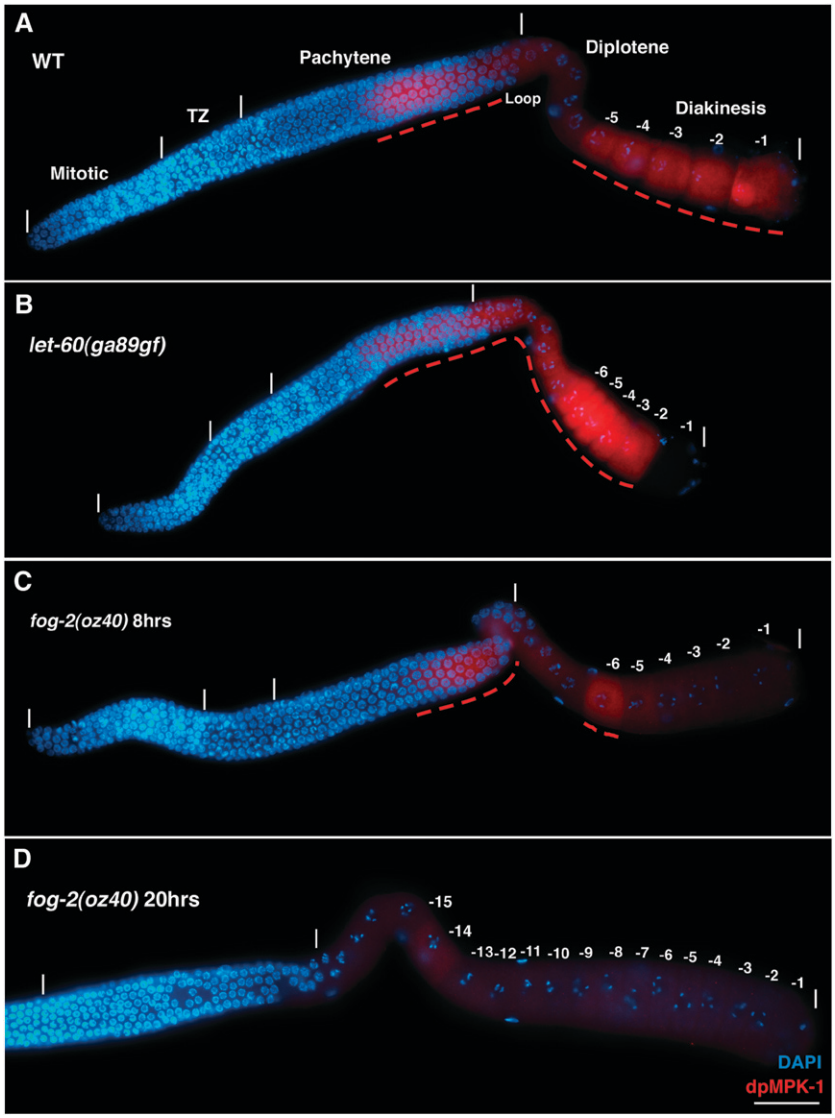

Figure 2.—Dynamic temporal/spatial activation of MPK-1 during oogenesis. Animals of the indicated genotype were grown at 20°, and the gonads were dissected and stained for activated dpMPK-1 (in red) and chromosome morphology (DAPI in blue). In A–D, distal is to the left and proximal is to the right; germline regions deduced from chromosome morphology (*e.g.*, pachytene) are indicated with the boundaries of the regions, the distal tip and proximal ends of the germline marked by vertical white lines; and panels with composite micrographs show a surface view distal to the loop and an interior view at the level of oocyte nuclei proximal to the loop. Dashed red lines indicate elevated dpMPK-1 staining. (A) Wild-type (WT) hermaphrodite germline 24 hr post mid-L4. High dpMPK-1 levels are observed in proximal pachytene and in the -1 through -5 diakinesis oocytes with a low but detectable valley in the loop/diplotene. dpMPK-1 is not detected in the mitotic, transition zone, or distal pachytene regions. (B) *let-60(ga89gf)* hermaphrodite germline 24 hr post mid-L4 at 20°, stained, and photographed together with A; images were processed identically. dpMPK-1 rises earlier in pachytene, remains elevated in the loop/diplotene, and is further elevated in diakinesis oocytes. dpMPK-1 falls abruptly as the -1 oocyte undergoes maturation in *let-60(ga89gf)* as it does in wild type (Figure 4C). (C) *fog-2(oz40)* female germline 8 hr after synchronization at the L4/adult molt, stained, and photographed together with A and B, but with a 2.5× exposure time, followed by identical image processing. dpMPK-1 is observed in proximal pachytene as in wild type and a single diakinesis oocyte, -6. Similar results were obtained with young *fog-3(q443)* females. (D) *fog-2(oz40)* female germline 20 hr post L4/adult molt containing >15 oocytes arrested in diakinesis (distal-most region not shown). Very low or undetectable dpMPK-1 is observed in proximal pachytene, diplotene, and diakinesis. Not shown is dpMPK-1 accumulation (1) in sheath cell nuclei, which is weak in wild type and elevated in *let-60(ga89gf)*, and (2) in a subset of intestinal cells (nucleus and cytoplasm), which is low in wild type and elevated in *let-60(ga89gf)*.

one mRNA target, *cep-1*, begins and CEP-1 p53 is detected in late proximal pachytene nuclei (Schumacher *et al.* 2005), while in diplotene, when GLD-1 levels are very low, translation of another target mRNA, *rme-2*, occurs and the RME-2 yolk receptor is detected (Lee and Schedl 2001). In *mpk-1* null germlines, GLD-1 levels remain elevated throughout the extended pachytene region and nuclear CEP-1 as well as RME-2 fail to accumulate (supplemental Figure 3 at http://www.genetics.org/supplemental/; Lee and Schedl 2004; Leacock and Reinke 2006), again indicating that the arrested pachytene cells do not display late proximal pachytene character.

To further investigate the arrest point relative to the distal pachytene region, we examined polarization of meiotic nuclei. In leptotene/zygotene, as homologous chromosomes pair and synapse, nuclei have a distinctive polarized appearance with the chromosomes and nucleolus displaced toward opposite sides (MacQueen and Villeneuve 2001). This polarized arrangement continues through the distal-most one-fourth/one-third of pachytene in a region termed "early pachytene" with later stage pachytene nuclei showing a symmetric/dispersed organization (Carlton *et al.* 2006). Analysis of *mpk-1* null hermaphrodite germlines for DNA morphology and nucleolar position, using anti-NOP-1 antibody staining (MacQueen and Villeneuve 2001), revealed that *mpk-1(ga117)*-arrested pachytene nuclei have a symmetric chromosome and nucleolar organization (data not shown), demonstrating that they have progressed beyond the early pachytene polarized organization. Together, the marker staining and nuclear

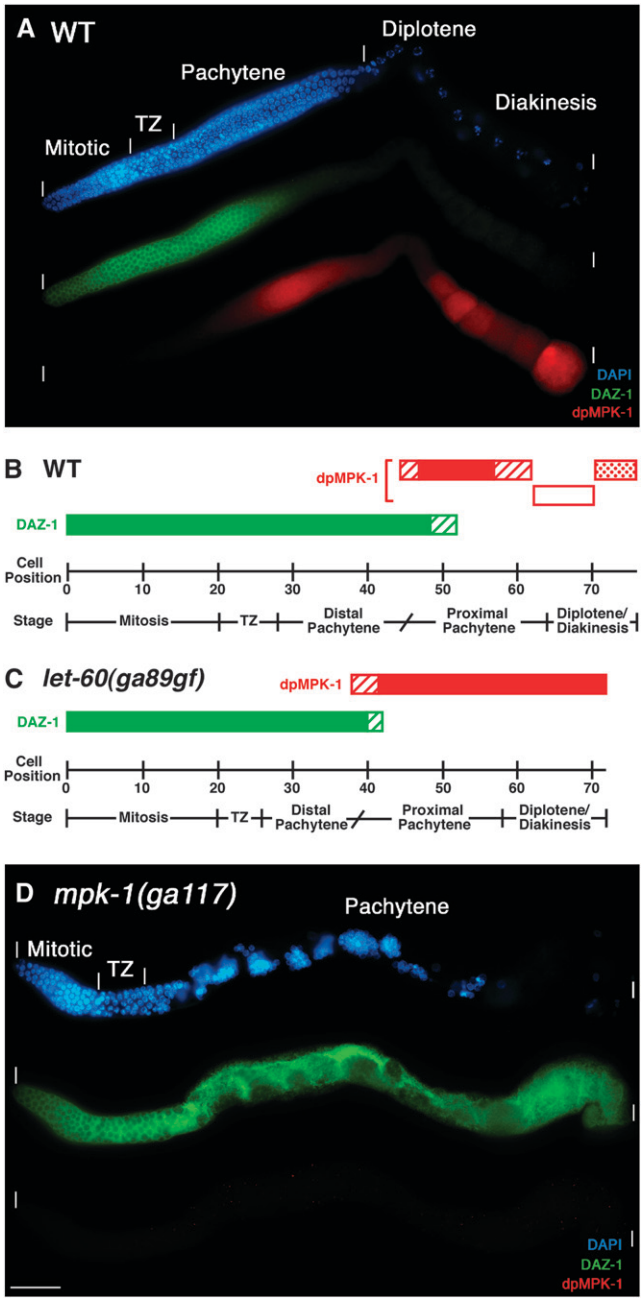

FIGURE 3.—MPK-1 is necessary for progression from distal to proximal pachytene. Wild-type, *let-60(ga89gf)*, and *mpk-1(ga117)* hermaphrodites at 20° were dissected 24 hr post mid-L4 and stained for DAZ-1 (green), dpMPK-1 (red), and chromosome morphology (DAPI in blue). (A) In wild type, DAZ-1 is high in the mitotic and transition zone and falls in mid-pachytene. (B) Representation of the cellular positions for DAZ-1 (green) and dpMPK-1 (red) accumulation in cell diameters from the distal tip from visual inspection of 13 wild-type germlines. Solid bars indicate high levels of DAZ-1 or dpMPK-1, diagonal-line bars indicate rising or falling levels, the open bar indicates lower dpMPK-1 accumulation at the end of pachytene and in diplotene, and the stippled bar indicates variable high dpMPK-1 accumulation in diakinesis oocytes. The fall of DAZ-1 is reciprocal to the rise in dpMPK-1 accumulation, with a region of overlap of ~7 cell diameters. Stages, separated by a vertical line, are determined from DAPI morphology while a diagonal line is used to separate distal pachytene from proximal pachytene as it is inferred from the rise in dpMPK-1 staining. (C) Representation of the cellular positions for DAZ-1 and dpMPK-1 accumulation from nine *let-60(ga89gf)* germlines (stained germline not shown). dpMPK-1 levels rise prematurely, DAZ-1 levels fall prematurely, and the pachytene region is 5 cell diameters shorter than that of wild type, consistent with the hypothesis that the rise in dpMPK-1 promotes a transition from distal to proximal pachytene. (D) In *mpk-1(ga117)* null germlines, pachytene-arrested germ cells are found in the proximal two-thirds of the gonad and display distal/mid-pachytene character based on a high DAZ-1 level. dpMPK-1 is not detected. Due to massive disorganization, cellular positions were not determined.

morphology indicate that *mpk-1* null germ cells arrest with mid-pachytene characteristics, at approximately the same point at which dpMPK-1 levels would normally rise. On the basis of these results we propose that MPK-1 promotes pachytene progression, with the rise in dpMPK-1 triggering a transition from a distal pachytene to a proximal pachytene subtype (Figure 3B).

dpMPK-1 and pachytene progression in select mutant backgrounds: To understand the relationship between dpMPK-1 levels and pachytene progression, we examined mutants in the *let-60* RAS–*mpk-1* ERK pathway, sex determination mutant females, and mutants in which initiation of meiotic recombination is blocked. The canonical *let-60* RAS gf allele *n1046*, which has a strong effect on vulval development (BEITEL *et al.* 1990; HAN *et al.* 1990), is fertile at 15°, 20°, and 25° and has a dpMPK-1 accumulation pattern that is indistinguishable from wild type (Table 3 legend). By contrast, the *let-60* gf allele *ga89*, which has a relatively mild effect on vulval development (EISENMANN and KIM 1997), causes ts sterility and alters dpMPK-1 accumulation (Table 3; Figures 2B and 3C; supplemental Figure 4 at http://www.genetics.org/supplemental/). *let-60(ga89gf)* hermaphrodites are fertile at 20° but show earlier/more distal MPK-1 activation. Comparison of wild-type and mutant hermaphrodites 24 hr post L4 at 20° reveals that dpMPK-1 rises at 38 (±3) cell diameters from the distal tip in *let-60(ga89gf)* compared to 45 (±3) cell diameters in wild type. However, overall *let-60(ga89gf)* germlines are 4 cell diameters shorter than wild type in distal–proximal length (72 ± 3 *vs.* 76 ± 2) and the pachytene region is 5 cell diameters shorter (32 ± 2 *vs.* 37 ± 2). Therefore, we used percentage of length through pachytene where dpMPK-1 begins to rise as a way to normalize for differences in cell diameter length of pachytene and total germline. dpMPK-1 rises at ~37% of the length of pachytene in *let-60(ga89gf)* compared to ~46% of length in wild type. Although the rise in dpMPK-1 occurs prematurely in *let-60(ga89gf)*, the peak level of dpMPK-1 in pachytene, as judged by pixel intensity, is similar to wild type (supplemental Figure 4). The premature rise in dpMPK-1 suggests that the

TABLE 1

Strong loss-of-function alleles of *mpk-1*, *mek-2*, and *lin-45* display the same germline phenotypes

		% gonad arms with indicated phenotype[a]						
Genotype	Hr after L4	Disrupted pachytene cellular organization	Pachytene arrest[b]	Normal oocytes	Normal sperm	Normal dpMPK-1	Mitotic zone size[c]	*n*
Wild type[d]	18	0	0	100	100	100	18 ± 1.4	24
mpk-1(ga117)[d]	18	100	100	0	0	0	19 ± 3.2	39
	42	100	100	0	0	0	11 ± 2.0	37
mek-2(q425)[d]	18	100	100	0	0	0	19 ± 3.0	39
	42	100	100	0	0	0	10 ± 1.9	33
Wild type[e]	18	0	0	100	100	100	21 ± 1.6	24
lin-45(dx19)[e]	18	100	100	0	0	0	21 ± 3.4	39
	42	100	100	0	0	36[f]	14 ± 2.8	50

[a] L4 hermaphrodites of the indicated genotype were picked and scored at the indicated later times. Null alleles *mpk-1(ga117)* and *lin-45(dx19)* are described in Lackner and Kim (1998) and in Hsu *et al.* (2002), respectively, and the strong lf allele *mek-2(q425)* in Church *et al.* (1995). The phenotypes are described in text.

[b] Proximal nuclei that would normally form sperm or oocytes are arrested in pachytene. Pycnotic nuclei are often observed among pachytene nuclei in all three genotypes; the basis of this phenotype is not known.

[c] Number of cell diameters from the distal tip cell to the first transition zone nucleus observed from DAPI staining, plus or minus the standard deviation (similarly for Tables 2 and 3). From subsequent examinations of a large number of *mpk-1(ga117)* germlines, we observed polyploid nuclei in ~5–10% of mitotic zones as well as a few percent where the mitotic zones contain only a few germ cells.

[d] Indicated strains contain *unc-32(e189)*.

[e] Indicated strains contain *unc-5(e53)*.

[f] Staining pattern is abnormal and limited to the most proximal region (supplemental Figure 2 at http://www.genetics.org/supplemental/). Also see supplemental Figure 1 legend for discussion of dpMPK-1 in *lin-45* mutants.

transition from distal to proximal pachytene occurs earlier in *let-60(ga89gf)* germlines and leads to the prediction that DAZ-1 levels should fall prematurely in the mutant. We found that DAZ-1 levels terminate earlier at 42 (±2) cell diameters from the distal tip, corresponding to ~51% of the length, in *let-60(ga89gf)* germlines compared to terminating at 52 (±3) cell diameters or 67% of pachytene length in wild type (Figure 3, B and C). The results with *let-60(ga89gf)* are consistent with the proposal that the rise in dpMPK-1 promotes the transition of germ cells from a distal pachytene subtype to a proximal pachytene subtype. The decrease in size of the pachytene region in *let-60(ga89gf)* may be a consequence of the premature rise in dpMPK-1, assuming that the distal-to-proximal transition is rate limiting.

In an attempt to further perturb pachytene progression, we examined *let-60(ga89gf)* mutants shifted to the restrictive temperature. After a 4-hr shift of *let-60 (ga89gf)* adults to 25°, animals become sterile due to

TABLE 2

Phenotypes following shift-up of *mpk-1(ga111)* to 25°

	% hermaphrodite gonad arms with indicated phenotype									
	Pachytene cellular organization									
Genotype	Gaps in sheet of cells	Internal cells/nuclei	Pycnotic nuclei[a]	Proximal pachytene nuclei	Normal diakinetic nuclei	Disorganized oocytes	Emo	Normal sperm	Mitotic zone size	*n*
				Embryo shift-up						
Wild type	0	0	0	0	100	0	0	100	18 ± 2.1	22
mpk-1(ga111)	97	41	84	91	19	9	16	97	18 ± 2.3	32
				L4 shift-up						
Wild type	0	0	0	0	100	0	0	100	19 ± 1.8	22
mpk-1(ga111)	94	6	0	66	66	16	41	97	19 ± 2.6	32

The temperature-sensitive *mpk-1(ga111)* is described in Lackner and Kim (1998). Animals were collected for gonad dissection 24 hr post L4 at 25°.

[a] Pycnotic nuclei can contain HIM-3 aggregates.

TABLE 3

Phenotypes of *let-60(ga89gf)*

Genotype	% hermaphrodite gonad arms with indicated phenotype: Oocyte phenotypes: Disorganized	Small oocytes, multiple rows	Emo	Ectopic dpMPK-1	Mitotic zone size[c]	*n*
			20°[a]			
Wild type	0	0	0	0	21 ± 1.8	20
let-60(ga89gf)	10	0	0	100	21 ± 1.6	30
			25° shift-up[b]			
Wild type	0	0	0	0	21 ± 1.6	20
let-60(ga89gf)	40	60	17	100	20 ± 1.5	30

let-60(ga89gf) is described in Eisenmann and Kim (1997). *let-60(n1046gf)* (Beitel *et al.* 1990; Han *et al.* 1990) hermaphrodites were also examined: First, mutant hermaphrodites are fertile at 15°, 20°, and 25°. At 20°, 58% of gonad arms have a mild disorganized oocyte phenotype ($n = 31$). At all temperatures, mutants lay small embryos. Time-lapse video analysis at 20° shows that the small embryos primarily arise from premature closure of the proximal gonad/distal spermathecal valve, resulting in the maturing oocyte being chopped during ovulation into the spermatheca. Second, the levels and spatial pattern of dpMPK-1 are similar in *let-60(n1046gf)* and wild type (see supplemental Figure 5 at http://www.genetics.org/supplemental/).

[a] Animals were picked at mid-L4 and 24 hr later gonads were obtained by dissection.

[b] Animals were picked at mid-L4, grown for an additional 20 hr at 20°, and shifted to 25° for 4 hr; then gonads were obtained by dissection.

[c] Length of the mitotic zone, in cell diameters from the distal tip, on the basis of DAPI nuclear morphology.

defects in oocyte growth and differentiation (Table 3, see below). dpMPK-1 in the pachytene region is increased in level from 20° but does not extend farther distally and can show variability even within the same gonad (data not shown). The size of the pachytene region following a 4-hr shift to 25° is not significantly different from that at 20°. Shifts of *let-60(ga89gf)* for >4 hr were not informative as mutants accumulate large amounts of fluid in the pseudocoelom (the Clr phenotype; Huang and Stern 2004), which leads to secondary gonadal phenotypes, including shriveled germlines and complete loss of dpMPK-1 staining.

We examined MPK-1 activation and pachytene progression in sex determination mutant females, which do not mature and ovulate oocytes in the absence of the sperm-derived MSP signal (McCarter *et al.* 1999; Miller *et al.* 2001). Adult females that contain > ~15 oocytes in the proximal gonad have a normal-size pachytene region and have low dpMPK-1 staining in both pachytene and proximal oocytes, which is restored following mating with wild-type males (Figure 2D; Miller *et al.* 2001; Page *et al.* 2001; data not shown). One interpretation of these results is that pachytene progression does not require activated MPK-1 and that MSP/sperm signaling is necessary for MPK-1 activation in pachytene. However, in adult females, new oocytes are generated at a very low rate and germ cells progress through pachytene significantly slower than in hermaphrodites (see below; Jaramillo-Lambert *et al.* 2007). We therefore examined dpMPK-1 staining in young adult females that are generating new oocytes (see below) and observed MPK-1 activation in pachytene similar to wild type, although with reduced intensity (Figure 2C). Thus activation of MPK-1 in proximal pachytene is observed in young females where pachytene progression/oocyte formation is occurring and this activation is not MSP/sperm dependent.

We investigated whether MPK-1 activation and pachytene progression are affected by a failure to initiate meiotic recombination due to mutations in *spo-11* and *mre-11*, two genes necessary for double-strand break (DSB) formation (Dernburg *et al.* 1998; Chin and Villeneuve 2001), or loss of *mrt-2*, a gene necessary for DNA-damage-induced apoptosis/pachytene recombination checkpoint (Gartner *et al.* 2000). Analysis of these mutants showed that the extent of dpMPK-1 staining and the proportion of pachytene-stage germ cells compared to total germ cells was not different from wild type (supplemental Figure 5, A and B, at http://www.genetics.org/supplemental/). Conditions that impair homologous chromosome synapsis cause a delay in reorganization of pachytene chromosomes to the symmetric/dispersed configuration and this delay is suppressed by preventing DSBs with a *spo-11* null mutation (Carlton *et al.* 2006). To test whether the pachytene-arrest phenotype of *mpk-1* mutants might be caused by a defect in chromosome synapsis, we examined the phenotype of *mpk-1(ga111); spo-11(ok79)* at 25° and stained *mpk-1(ga117)* mutants with anti-HIM-3 antibodies, which marks the axis of paired chromosomes. We found that blocking double-strand break formation failed to suppress the pachytene-arrest phenotype (data not shown) and that HIM-3 staining is normal in *mpk-1* null germlines (supplemental Figure 6H), suggesting

that the pachytene-arrest phenotype is unlikely to be caused by a defect in meiotic chromosome synapsis.

MPK-1 is necessary for pachytene cell organization: Previous work reported that pachytene-arrested nuclei in *mpk-1*, *mek-2*, *ksr-2*, and *let-60* lf mutants are present in clumps on the basis of Nomarski microscopy and DAPI staining (Church *et al.* 1995; Ohmachi *et al.* 2002). To understand the basis of this phenotype, we examined the organization of the germline using antibodies to Syntaxin 4 (SYN-4) and Patched-1 (PTC-1) to visualize cell membranes (Jantsch-Plunger and Glotzer 1999; Kuwabara *et al.* 2000) and rhodamine–phalloidin (R-ph) to visualize actin filament organization (Strome 1986). In wild type, these cytological reagents show that from the mitotic region through the end of pachytene, germ cells are arranged in a honeycomb pattern on the surface of the cylindrical gonadal tube, with an interior nucleus/germ-cell-free rachis (Figure 1, B and D; supplemental Figure 6, A and E, at http://www.genetics.org/supplemental/; Hirsh *et al.* 1976; Hall *et al.* 1999; Maddox *et al.* 2005). By contrast, SYN-4 and PTC-1 staining in *mpk-1* and *lin-45* null and *mek-2* strong lf mutant hermaphrodite germlines reveals a complete loss of the honeycomb organization of surface pachytene cells and the interior rachis; the gonadal tube is shrunken and distorted, the majority of the surface of the germline is devoid of germ cells, and instead nuclei and associated membranes are found in disorganized clumps (Table 1; supplemental Figure 6, B–D). Large regions that are devoid of nuclei and organized membranes are apparently cytoplasm as they contain cytoplasmic DAZ-1 and GLD-1 that are relatively uniformly distributed (Figure 3D; supplemental Figure 3A). In wild type, cortical actin is organized in a honeycomb pattern that mirrors membranes (Strome 1986), while in the rachis there is a fine filament network (Wolke *et al.* 2007). In strong *mpk-1*, *mek-2*, and *lin-45* mutant hermaphrodite germlines, the pachytene actin organization is completely disrupted, with areas lacking organized filaments and cytoplasmic regions that contain macroscopic aggregates of actin (supplemental Figure 6F). In these strong mutants, the cellular disorganization progresses distally in older animals and can extend into distal pachytene and the transition zone, regions where dpMPK-1 is not detected. It is unclear whether the disorganization of transition zone and distal pachytene germ cells is due to a requirement of MPK-1 function in these regions or whether it is a secondary consequence of massive disruption of the more proximal germline that spreads distally. Under conditions of partial *mpk-1* lf, either shift-up of *ga111* to 25° or following *mpk-1* RNAi (see below), disruptions of pachytene germ cell organization are less severe, including gaps in the honeycomb pattern and the presence of internal nuclei in the rachis (Table 2; supplemental Table 1). Together, these results indicate that MPK-1 is necessary for the organization of the pachytene region into germ cells on the surface of the gonadal tube and an interior cytoplasmic rachis.

Dynamic dpMPK-1 accumulation in the proximal germline: As germ cells progress from proximal pachytene to growing diplotene oocytes in the loop region, dpMPK-1 falls to low but detectable levels (Figures 1A, 2A, and 3, A and B). dpMPK-1 then rises in late-stage diakinesis oocytes, with the most proximal approximately five oocytes (-1 to -5) staining strongly. However, the levels are variable from oocyte to oocyte and from gonad to gonad, with oocytes at the same position showing large differences in dpMPK-1 level. This variability in proximal oocyte dpMPK-1 level is illustrated qualitatively in Figure 4A, based on a large sample of gonads scored (supplemental Figure 7 at http://www.genetics.org/supplemental/), and quantitatively from determination of oocyte pixel intensity (supplemental Figure 8). Although there is not a clear pattern of dpMPK-1 level relative to oocyte position from examination of fixed specimens, it is possible that the dynamic pattern reflects some yet-to-be-defined stage/process of oocyte development. The exception is the -1 oocyte where dpMPK-1 levels are correlated with the stage of meiotic maturation. The -1 oocyte in hermaphrodites spends ~23 min in the most proximal position and in the final 3–6 min will undergo the meiotic maturation events of nuclear envelope breakdown (NEBD) and cortical rearrangement (McCarter *et al.* 1999; Figure 6). During this period, the initially dispersed diakinesis bivalents of the -1 oocyte congress to the metaphase plate, chromosomal AIR-2 aurora kinase staining increases from low to high and metaphase I (MI) spindle formation begins (Figure 4, B and C; Schumacher *et al.* 1998; Rogers *et al.* 2002; Yang *et al.* 2003). We found that in ~15% of -1 oocytes dpMPK-1 is very low/undetectable (Figure 4, A and C). Comparing -1 oocyte stage with dpMPK-1 level, we found that 100% of early -1 oocytes (dispersed diakinesis bivalents, low chromosomal AIR-2 staining) have high dpMPK-1 while >85% of late -1 oocytes (congressed bivalents, high chromosomal AIR-2 staining) have very low dpMPK-1 (Figure 4, B and C; supplemental Table 2). This is consistent with observations of Page *et al.* (2001) who reported that, by completion of MI, dpMPK-1 is not detectable. Thus, as the -1 oocyte undergoes maturation, there is a rapid and dramatic fall in dpMPK-1 level.

Examination of dpMPK-1 levels in *let-60(ga89gf)* at 20° as germ cells progress from proximal pachytene to growing diplotene oocytes reveals that levels remain elevated rather than decrease in the loop region as is observed in wild type (Figure 1A; Figure 2, A and B; supplemental Figure 8 at http://www.genetics.org/supplemental/). In the most proximal, approximately eight diakinesis oocytes, dpMPK-1 levels are further elevated relative to wild type, as shown quantitatively from pixel intensity per oocyte (supplemental Figure 8). Notwithstanding the elevated dpMPK-1 levels in proxi-

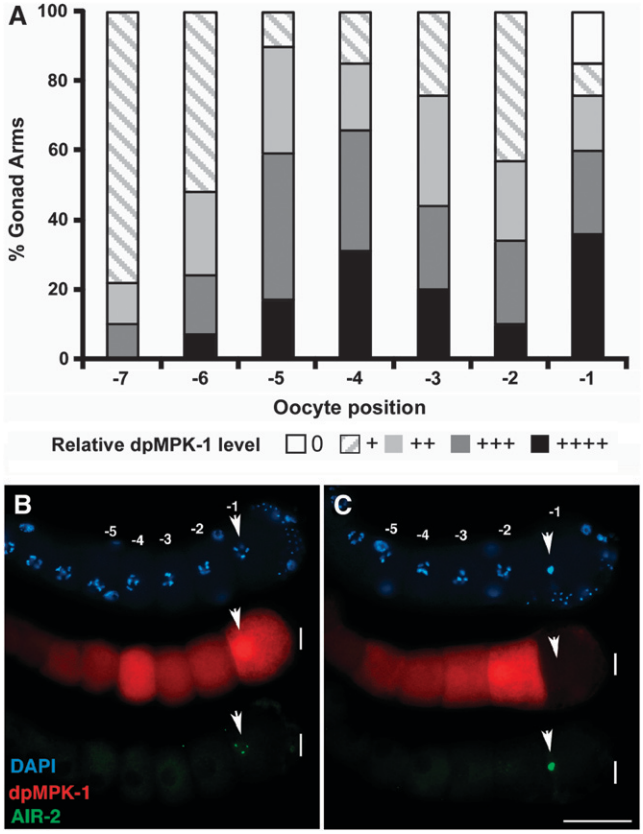

Figure 4.—Dynamic/variable MPK-1 activation in diakinesis oocytes. (A) Bar graph showing qualitative scoring of dpMPK-1 levels in proximal oocytes (-1 through -7) from 51 wild-type germlines following dissection 24 hr post mid-L4. Supplemental Figure 7 at http://www.genetics.org/supplemental/ contains a subset of the germlines used and illustrates the qualitative scoring for relative dpMPK-1 level (from undetectable at 0 to peak intensity at ++++) used to generate the graph. Quantitative measurements of pixel intensity from three germlines provide a fully consistent data set (supplemental Figure 8A). The proximal -1 through -5 oocytes in general display high dpMPK-1 accumulation although levels vary significantly for oocytes within the same gonad. Unlike the more distal oocytes, ~15% of -1 oocytes have very low/undetectable dpMPK-1. Not shown is cytoplasmic CGH-1 staining, which was used to assess germline damage during dissection (which might cause spurious reduction in dpMPK-1 level). (B and C) MPK-1 activation falls to undetectable levels as the -1 oocyte undergoes meiotic maturation. Wild-type hermaphrodites 24 hr post mid-L4 were dissected and stained for dpMPK-1 (red), AIR-2 aurora kinase (green), and chromosome morphology (DAPI in blue). Only oocytes late in the ~23 min time line of maturation/ovulation, as judged by prometaphase DAPI staining and high AIR-2 accumulation on chromosomes, show low or absent dpMPK-1 accumulation. Arrows indicate the position of the DAPI- and AIR-2-stained chromosomes in the -1 oocyte.

mal *let-60(ga89gf)* oocytes, we observe the same dramatic fall in the maturing -1 oocyte (Figure 2B).

To determine whether the generation of new oocytes influences dpMPK-1 accumulation, we compared younger and older adult females. In adult females, >20 hr post mid-L4, which contain >15 late-stage oocytes arrested in diakinesis and generate new oocytes at a very low rate, dpMPK-1 staining in oocytes is very low, lower than in diplotene oocytes in wild-type hermaphrodites (Figure 2D; McCarter *et al.* 1999; Miller *et al.* 2001; Page *et al.* 2001). In younger females, however, on average a single diakinesis oocyte reproducibly shows dpMPK-1 staining (Figure 2C; supplemental Figure 9 at http://www.genetics.org/supplemental/) at an intensity similar to diplotene or early diakinesis in wild-type hermaphrodites. In these young females, new late-stage diakinesis oocytes are being generated: at 6 hr after the L4/adult molt, there are on average 5.8 oocytes while at 8 hr there are 8.7 oocytes, a rate of oocyte production similar to young adult hermaphrodites prior to the first maturation/ovulation (McCarter *et al.* 1999; see supplemental Figure 9). The dpMPK-1-staining oocyte is on average at position -4.7 at 6 hr and at -7.4 at 8 hr, corresponding to the second oocyte proximal to the last diplotene oocyte. Thus, in young females, oocytes that have recently progressed to diakinesis activate MPK-1. The early diakinesis activation in females is apparently transient as only 80% of oocytes at this position accumulate dpMPK-1, and oocytes proximal or distal to this position in general do not stain. It is unclear if this MSP/sperm-independent activation of MPK-1 is specific to young females as oocytes in the same position in hermaphrodites show a similar or higher level of dpMPK-1. Instead, this early diakinesis activation may occur under situations where new late-stage oocytes are being generated.

MPK-1 function in oocyte organization and growth: The dynamic accumulation of dpMPK-1 in the proximal germline suggests that MPK-1 has functions during late oogenesis. However, in null/strong lf *mpk-1*, *mek-2*, and *lin-45* mutants, germ cells arrest in pachytene, precluding analysis of subsequent functions in oogenesis. Therefore, we have used temperature shifts of *mpk-1 (ga111)* and partial *mpk-1* RNAi to uncover functions during late oogenesis.

In wild-type hermaphrodites, as nuclei progress from pachytene to diplotene in the loop region, they form a single-file row on the external side while the rachis extends into the proximal gonad on the interior side. Oocyte volume progressively increases with corresponding plasma membrane growth that eventually fully encloses late-stage diakinesis oocytes. In *mpk-1(ga111)* shift-ups and in *mpk-1* RNAi, we observed a constellation of phenotypes during oocyte formation that we call "disorganized oocytes": (1) instead of a single-file row of growing oocytes on the external surface, some oocytes are displaced to the internal surface, resulting in two or more oocytes partially overlapping at the same position and such mis-positioned oocytes usually do not have the normal cylindrical shape; (2) instead of a progressive increase in oocyte size, smaller oocytes are sometimes proximal to larger oocytes; and (3) oocytes occasionally contain two or three nuclei and, correspondingly, there

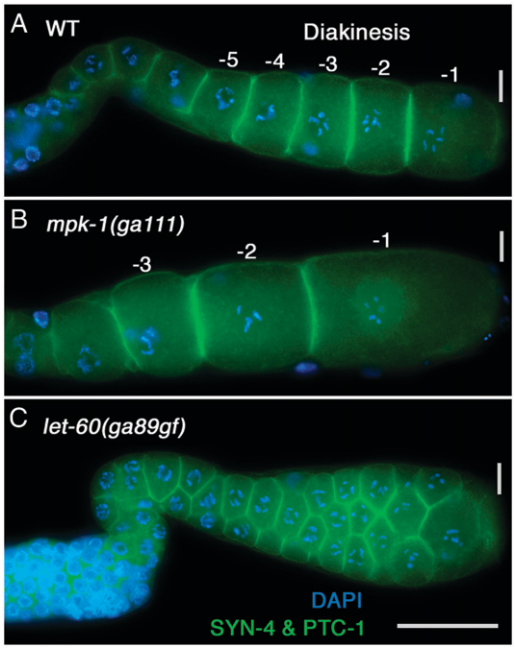

Figure 5.—MPK-1 activity has reciprocal effects on oocyte growth. (A) Wild-type and (B) temperature sensitive *mpk-1(ga111)* hermaphrodites were grown 16 hr post mid-L4 at 20°, shifted to 25° for 8 hr, and then dissected and stained for SYN-4 and PTC-1 (green) to visualize plasma membranes and DAPI (blue) to visualize chromosome morphology. Using surface area as a surrogate for volume, we found that reduction of *mpk-1* activity results in the -1 through -3 oocytes being larger than the corresponding oocytes in wild type (see supplemental Figure 10 at http://www.genetics.org/supplemental/ for quantitation). It is not currently known if the large oocyte phenotype also occurs in the absence of MSP/sperm. (C) *let-60(ga89gf)* hermaphrodites were grown 20 hr post mid-L4 at 20°, shifted to 25° for 4 hr, and then dissected and stained as above. The proximal germline contains small oocytes, variable in size, with multiple oocytes at a given distal–proximal position.

are small membrane-enclosed regions that lack nuclei, often on the interior side (Table 2; supplemental Table 1 at http://www.genetics.org/supplemental/; data not shown). As the formation of the single-file assembly line of oocytes occurs after pachytene, we wondered if the disorganized oocyte phenotype in *mpk-1(ga111)* and *mpk-1* RNAi germlines could be a secondary consequence of prior disruption of the organization of pachytene germ cells. This seems not to be the case as we find germlines with the disorganized oocyte phenotype while pachytene cell organization and pachytene progression are unaffected. Thus *mpk-1* function in oocyte organization and differentiation appears to be distinct from the distal germline functions in pachytene cellular organization and pachytene progression.

We also examined a series of shorter *mpk-1(ga111)* shift-ups, which likely result in less reduction in MPK-1 activity than the 24-hr shift-up or continuous growth at 25°. In 8-, 9-, or 10-hr shift-ups, two striking oocyte phenotypes were observed (Figure 5). First, the -1 through -3 oocytes were significantly larger than wild type; using surface area as a proxy for volume, the -1 and -2 *mpk-1(ga111)* oocytes were about twice the wild-type size (supplemental Figure 10 at http://www.genetics.org/supplemental/). Second, the nucleus of proximal oocytes, which in wild type migrates to the distal edge, is centrally located and fails to migrate (Figure 5). The large oocyte phenotype is unlikely to be a consequence of the disorganized oocyte phenotype that occurs distally as it was often observed in gonad arms that have an apparently normal single-file row of oocytes. That *mpk-1* might have a function in oocyte growth control is consistent with the previous observation of large oocytes in the *let-60* RAS pathway mutants *let-60(n1046dx1)* lf and *ptp-2* null (Church *et al.* 1995; Gutch *et al.* 1998).

To determine the effect of increasing MPK-1 activity as compared to wild type, we shifted *let-60(ga89gf)* adults to 25° for 4 hr. This results in small diakinesis oocytes, with two to four small oocytes at a given distal–proximal position (Table 3; Figure 5C; supplemental Figure 11C at http://www.genetics.org/supplemental/). Therefore, decreasing and increasing MPK-1 activity has opposite effects on oocyte size, suggesting that MPK-1 activity may control oocyte growth. While the only known function of LET-60 is to stimulate MPK-1 in *C. elegans* (Sundaram 2006), in other systems Ras can signal through downstream effectors that are distinct from ERK (Vojtek and Der 1998), opening the possibility that in the shift-up *let-60* is working through another effector in addition to MPK-1. In adult females, dpMPK-1 levels are low in pachytene, diplotene, and diakinesis. To test whether the small oocyte phenotype in *let-60(ga89gf)* shift-up is the result of high dpMPK-1 levels, we examined the phenotype of *fem-3(e1996) let-60(ga89gf)* adult females shifted to 25° for 4 hr. We found that, while dpMPK-1 staining was detected in pachytene, levels were uniformly low in diplotene and diakinesis, although occasionally some diakinesis oocytes showed strong staining (supplemental Figure 11 and data not shown). The small oocyte phenotype is strongly suppressed in the double mutant as we observe a single row of normal-size oocytes. This suppression suggests that, in the *let-60(ga89gf)* single mutant at 25°, high dpMPK-1 leads to the small-oocyte phenotype. However, a caveat is that *fem-3(e1996) let-60(ga89gf)* adult females generate new oocytes at a low rate so it is possible that insufficient new oocytes are generated during the shift to 25° to observe the small-oocyte phenotype and/or that, once arrested in diakinesis, oocyte growth is immune to changes in *let-60 (ga89gf)* activity. In sum, the results from the *mpk-1 (ga111)* and *let-60(ga89gf)* shift-up experiments suggest that low MPK-1 activity promotes oocyte growth while high MPK-1 activity may inhibit oocyte growth.

MPK-1 functions in the germline for meiotic prophase progression and gametogenesis: dpMPK-1 is observed in both the germline and gonadal sheath cells (Figures

1A and 2A). Accordingly, MPK-1 might act in the germline, the soma, or both to control pachytene progression, pachytene cell organization, oocyte organization and differentiation, oocyte growth, and oocyte nuclear migration. Previously, mosaic analysis with a strong lf *mpk-1* mutant indicated that MPK-1 function in the germline is necessary for pachytene progression and pachytene cell organization (Church *et al.* 1995). *rrf-1* encodes an RNA-dependent RNA polymerase that is important for the RNAi response in somatic cells but not in germ cells (Sijen *et al.* 2001). To distinguish between germline and somatic function, we compared *mpk-1* RNAi in wild type with RNAi in the *rrf-1* null background. Pachytene arrest, pachytene cellular disorganization, disorganized oocytes, large oocytes, and defective oocyte nuclear migration were phenotypes observed following RNAi in both *rrf-1* null and in wild type (supplemental Table 1 at http://www.genetics.org/supplemental/). This indicates that *mpk-1* function in the germline is necessary for control of pachytene progression, pachytene cell organization, oocyte organization and differentiation, oocyte growth, and oocyte nuclear migration (summarized in the discussion and Table 4).

MPK-1 is required for timely oocyte meiotic maturation and ovulation: A role for MPK-1 in oocyte maturation and ovulation is suggested both by the presence of dpMPK-1 in late-stage oocytes of hermaphrodites and mated females undergoing maturation/ovulation and by the absence of dpMPK-1 and the maturation/ovulation in females that lack the MSP-derived sperm signal (McCarter *et al.* 1999; Miller *et al.* 2001). To determine if *mpk-1* has a function in maturation/ovulation, we examined the time line of landmark morphological events in late oocyte development and maturation/ovulation using time-lapse video microscopy of *mpk-1(ga111)* hermaphrodites at the restrictive temperature (Ward and Carrel 1979; McCarter *et al.* 1997). *mpk-1(ga111)* and wild-type hermaphrodites were picked at mid-L4, grown an additional 16 hr at 20° and shifted to 25° for 9 hr, followed by video recording at 23° or 24°. The time between successive maturations/ovulations in wild type averaged 24 min (Figure 6). By contrast, in *mpk-1(ga111)* it averaged 82 min or 3.6-fold slower in nine oocytes where successive maturations/ovulations were observed. The delay occurs prior to maturation as, once initiated, the events of maturation/ovulation (NEBD, cortical rearrangement, begin and end ovulation) occurred on the same time line as wild type (Figure 6). For three additional oocytes where a prior maturation/ovulation was observed, the subsequent maturation/ovulation failed to occur in >90 min of recording. These results suggest that MPK-1 activation is needed to fully transmit the MSP/sperm signal for oocyte meiotic maturation/ovulation. Under the partial lf conditions employed, germline morphology appeared normal with a single-file row of diakinesis oocytes, although oocytes were larger in size. Attempts to further decrease *mpk-1* function with longer shifts of mutant worms resulted in severe disruption of oocyte morphology (disorganized oocytes, etc.), precluding simple interpretation of results with these conditions. At 20°, *mpk-1(ga111)* germlines have essentially normal germline morphology, although the level of dpMPK-1 is lower than in wild type (supplemental Figure 12 at http://www.genetics.org/supplemental/). The large oocyte size appears not to be the cause of the maturation/ovulation defect at 25° since we also observed a delay in *mpk-1(ga111)* hermaphrodites at 20° where oocytes are of normal size (63 min between successive maturations/ovulations; data not shown). Thus, at a minimum, MPK-1 is necessary for triggering timely maturation/ovulation and in fact may be required to initiate the event.

If MSP sperm-dependent activation of MPK-1 is the trigger for maturation/ovulation, then one would predict that the point in the time line of landmark events at which oocytes are arrested in females should be the same as the mutant arrest following *mpk-1(ga111)* shift-up. This appears to be true. In females, oocytes are arrested after nuclear migration and prior to the events of maturation (NEBD and cortical rearrangement; McCarter *et al.* 1999). In *mpk-1(ga111)* shift-ups, oocytes are delayed or arrested prior to the events of maturation. One difference is that oocytes in *mpk-1(ga111)* shift-ups also display a failure of the nucleus to migrate to the distal edge. However, this likely reflects a distinct MPK-1-controlled process disrupted in the *mpk-1(ga111)* shift-up as, unlike MPK-1 function in maturation/ovulation, which is sperm dependent, MPK-1 function in oocyte nuclear migration is sperm independent as it occurs normally in females (McCarter *et al.* 1999). Interestingly, when females are briefly mated and examined shortly thereafter, the time between successive maturations/ovulations is only 11 min, compared to 24 min in hermaphrodites, with the events of maturation/ovulation occurring on the same time line as wild type (Figure 6). This timing difference suggests that in the hermaphrodite each -1 oocyte spends an additional ~12 min executing a process(s) that is completed during the prolonged oocyte arrest in adult females.

Further support for an MPK-1 function in maturation/ovulation comes from finding an endomitotic oocyte (Emo) phenotype in *mpk-1(ga111)* animals at 25° and following partial *mpk-1* RNAi in wild type and *rrf-1* (Table 2; supplemental Table 1 at http://www.genetics.org/supplemental/). Time-lapse analysis has shown that the Emo phenotype results when the oocyte undergoes maturation but ovulation fails, with the resulting unfertilized oocyte remaining in the gonad and undergoing endoreduplication cycles (Iwasaki *et al.* 1996; McCarter *et al.* 1997; Rose *et al.* 1997). The Emo phenotype observed with partial *mpk-1* lf suggests that maturation occurred normally but ovulation failed; however, until these intermittent/low-frequency events

A

Events	Wild-type	*mpk-1(ga111)**	*fem-3(e1996)* mated
1. End Nuclear Migration	-12.8 ± 6.1	No Migration	Migration Completed**
2. Nuclear Envelope Breakdown	-3.8 ± 0.6	-3.2 ± 1.2	-3.5 ± 0.7
3. Oocyte Cortical Rearrangement	-2.2 ± 0.6	-2.0 ± 1.0	-2.2 ± 0.3
4. Begin Ovulation	-0.7 ± 0.1	-1.0 ± 0.4	-0.9 ± 0.1
5. End Ovulation	0.0	0.0	0.0
6. Entry into Uterus	3.8 ± 0.3	3.7 ± 0.6	3.3 ± 0.6
7. Previous End Ovulation	-23.6 ± 3.7	-83.2 ± 30.4	-10.8 ± 1.9

* Not included are the three gonads where the -1 oocyte failed to mature and ovulate during the more than 90min of video analysis.

** In two cases, nucleus was displaced after ovulation of previous oocyte, but these nuclei quickly migrated to the distal end in the now -1 oocyte.

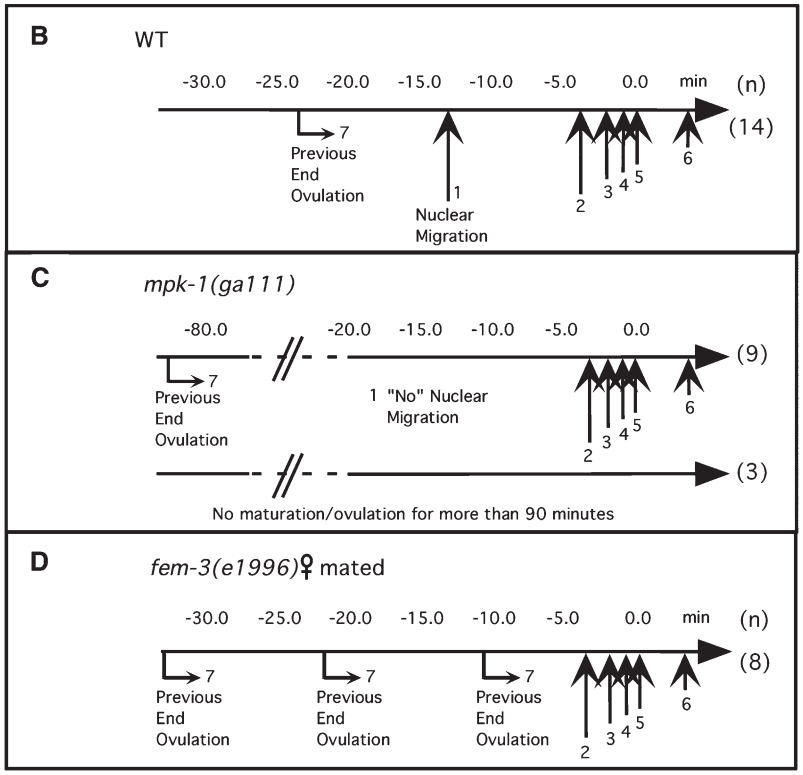

FIGURE 6.—MPK-1 is required for timely oocyte maturation/ovulation. The timing of landmark events of maturation/ovulation in the -1 oocyte was determined by Nomarski time-lapse video microscopy (see text and McCARTER *et al.* 1999). (A) Tabulation of the average timing of seven events (left column) for wild type ($n = 14$), *mpk-1(ga111)* ($n = 12$), and mated *fem-3(e1996)* females ($n = 8$) at 25°. "End Ovulation" (event 5) is defined as 0 min, earlier events (*e.g.*, event 1, "End Nuclear Migration") are given a negative time, and the interval between successive maturations ovulation is designated "Previous End Ovulation" (event 7). B–D are time lines for wild-type, *mpk-1(ga111)* and mated *fem-3(e1996)* females, respectively, derived from A, with vertical arrows showing the relative timing of each event. (B) For wild type, nuclear migration and the events of maturation/ovulation (arrows 2–5) occur as previously reported, with the interval between "Previous End Ovulation" (arrow 7) and "End Ovulation" (arrow 5) ~24 min. (C) For *mpk-1 (ga111)* ($n = 9$), there is a long delay between "End Previous Ovulation" and the events of maturation/ovulation. This delay is prior to the events of maturation/ovulation as, once initiated, they occur on the same schedule as wild type. The delay results in an ~83-min interval between successive maturations/ovulations, 3.6-fold slower than wild type. Nuclear migration was not observed. For three animals where a maturation/ovulation was observed at the beginning of the recording, a subsequent maturation/ovulation was not observed for >90 min. (D) Adult females, with oocytes arrested in diakinesis, were briefly mated with CB4855 ("Mr. Vigorous") males (HODGKIN and DONIACH 1997) and then recorded. Soon after mating, the interval between successive maturations/ovulations was reduced ~2-fold from that of wild type. The interval shortening occurs prior to the events of maturation/ovulation as, once initiated, they occur on the same schedule as wild type.

are examined by time-lapse microscopy, this interpretation is uncertain. Interestingly, an Emo phenotype is also observed in *let-60(ga89gf)* hermaphrodites shifted to 25° (Table 3); this presumably represents disruption of maturation/ovulation at a step separate from that observed in *mpk-1* lf.

MPK-1 ERK signaling is necessary for the male germ cell fate: In wild-type adult males, total MPK-1 is found in the mitotic region, the transition zone, and early pachytene but is no longer detectable by mid-pachytene (Figure 1C, supplemental Figure 13). dpMPK-1 is restricted to the proximal half of the transition zone and very early pachytene in an ~13-cell-diameter distal–proximal region (Figure 1C; Figure 7A). *mpk-1* null XO adult males display phenotypes very similar to null mutant hermaphrodites: nuclei are arrested in pachytene and the honeycomb pattern of germ cells on the surface of the cylindrical gonadal tube is disrupted, with regions of cytoplasm devoid of nuclei and cell membranes and little or no evidence of gametogenesis (Figure 7C; CHURCH *et al.* 1995; data not shown). These phenotypes suggest that MPK-1 functions to promote pachytene progression and pachytene cellular organization during spermatogenesis as it does in oogenesis. However, the MPK-1 expression pattern seems inconsistent with this possibility; dpMPK-1 accumulation in proximal pachytene in the hermaphrodite is likely to mediate pachytene progression and pachytene cellular organization during oogenesis, but during spermatogenesis dpMPK-1 is limited to the transition zone and very early distal pachytene and total MPK-1 is not detected in proximal pachytene.

An understanding of this discrepancy came from analysis of hermaphrodites with partial lf for *lin-45*, *mek-2*, and *mpk-1*. In animals that did not display pachytene arrest or pachytene cellular disorganization, a feminization of the germline phenotype was observed in which germ cells that would normally form sperm

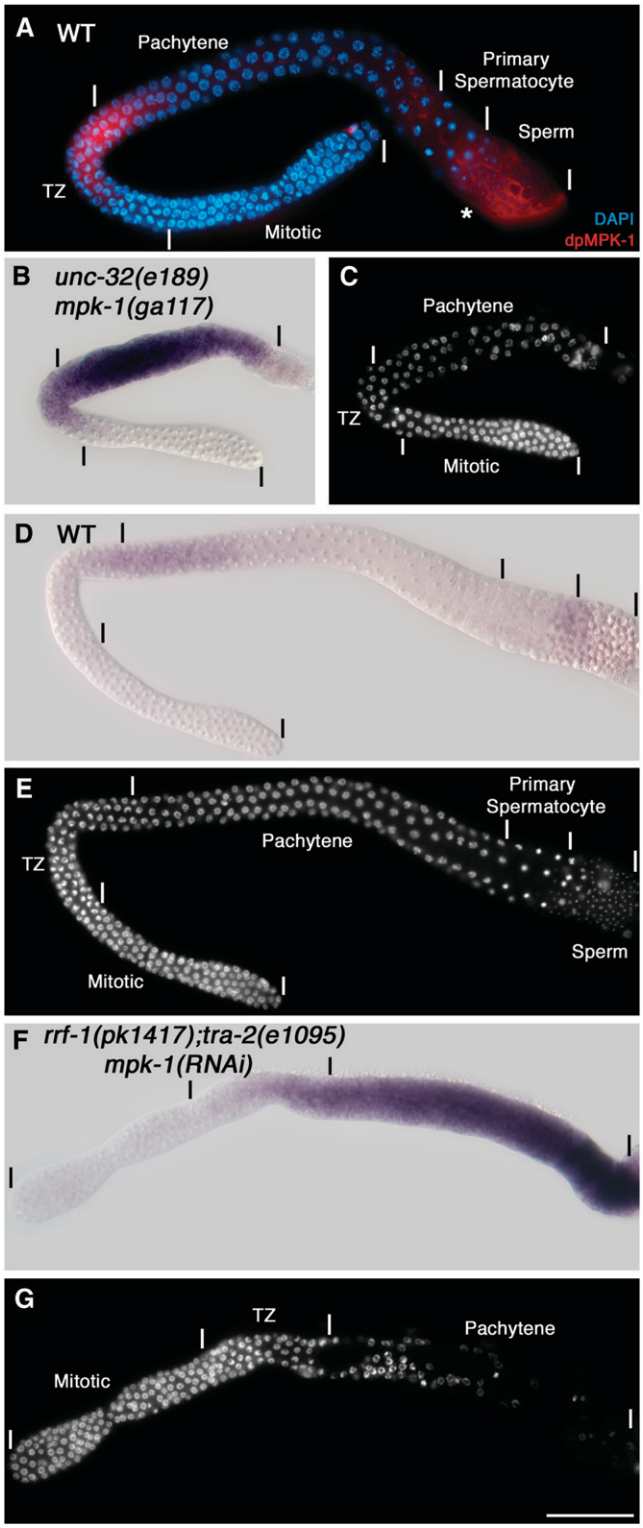

FIGURE 7.—MPK-1 is required for the male germ cell fate. (A) Wild-type adult males at 20° were dissected 24 hr post L4 and stained for dpMPK-1 (red) and chromosome morphology (DAPI in blue). dpMPK-1 is observed from the middle of the transition zone through early pachytene. Proximal dpMPK-1 staining in the region indicated with an asterisk corresponds to the vas deferens and likely is nonspecific as it is observed in *mpk-1(ga117)* null males. (B, D, and F) *In situ* hybridization of dissected gonads with yolk receptor *rme-2* antisense DNA (signal in purple) and the corresponding DAPI-stained germlines in (C, E, and G). (B and C) The *mpk-1(ga117) unc-32(e189)* adult male germline is feminized, showing a strong *rme-2* mRNA hybridization signal in the region where germ cells are disorganized and arrested in pachytene. (D and E) The wild-type adult male shows very low levels of *rme-2* accumulation. (F and G) The *rrf-1(pk1417); tra-2(e1095) null*; *mpk-1* RNAi adult male germline is feminized, showing a strong *rme-2* mRNA hybridization signal in the region where germ cells are disorganized and arrested in pachytene. We note that *mpk-1(ga117)* male germlines are smaller than those of wild type, at least in part because mutant males are sickly due to defective defecation; the defecation defect is not observed in *tra-2*; *mpk-1* double null mutant males.

instead form oocytes (supplemental Table 3 at http://www.genetics.org/supplemental/). On the basis of this partial lf phenotype, we speculated that, in *mpk-1* null males, the germline is fully feminized and thus would display the pachytene-arrest and pachytene cellular disorganization phenotypes observed in the absence of MPK-1 activity during oogenesis. We used two markers to test whether pachytene-arrested germ cells in males were feminized: *rme-2* mRNA and GLD-1 protein, which are present at high levels in pachytene of oogenesis but not of spermatogenesis (JONES *et al.* 1996; GRANT and HIRSH 1999; LEE and SCHEDL 2001). Consistent with a feminized phenotype, *in situ* hybridization shows that *rme-2* mRNA is expressed at high levels throughout the *mpk-1* null pachytene-arrested region compared with the near absence in control males (Figure 7, B–E). Hermaphrodites with strong lf mutations in *lin-45*, *mek-2*, and *mpk-1* also fail to make sperm (Table 1). The absence of sperm in these mutant hermaphrodites is also due to feminization. Proximal germ cells in mid-L4 gonads that would normally form sperm show high levels of *rme-2* mRNA in *mpk-1* null gonads in contrast to wild-type hermaphrodite gonads (supplemental Figure 14). We conclude that *lin-45*, *mek-2*, and *mpk-1* activities are necessary for the male germ cell fate in both hermaphrodites and males.

MPK-1 might act early to specify the sexual fate of all germ cells or might act continuously as germ cells transit from proliferation to meiotic development in larvae and adults. We used temperature shifts with *mpk-1(ga111)* to ask if there is an ongoing requirement for MPK-1 activity in specification of the male fate in males. *mpk-1(ga111)* males grown continuously at 15° have a normal male germline, yet have a feminized germline when grown continuously at 25°. When *mpk-1(ga111)* males grown at 15° until mid-L4—at which point they have begun spermatogenesis—are shifted to 25° for 24 hr, we observe feminization of the germline as assessed by sexually dimorphic high GLD-1 levels during pachytene of oogenesis (JONES *et al.* 1996; supplemental Figure 15 at http://www.genetics.org/supplemental/). To determine whether MPK-1 acts in germ cells or somatic cells to control germline sexual fate, we performed *mpk-1*

RNAi in the *rrf-1(pk1417)* background that is defective in somatic RNAi. The same level of feminization of the hermaphrodite germline was observed following *mpk-1* RNAi in wild type and *rrf-1* null (supplemental Tables 4 and S5), suggesting that *mpk-1* functions in the germline to control male fate.

Work from a number of groups has identified a pathway for specification of germline sexual fate (reviewed in Ellis and Schedl 2006). A set of genes that promotes the male fate, the genes *fem-1*, *-2*, and *-3* and *fog-1* and *-3*, act near the end of the pathway and are downstream of and inhibited by the *tra-2* gene, which promotes the female fate. We used genetic epistasis analysis to ask if *mpk-1* promotes the male fate by acting upstream or downstream/in parallel of *tra-2* in the sex determination pathway. *tra-2(e1095)* null XX mutants have a male germline and somatic gonad with the remaining soma almost fully masculinized (Hodgkin 1980). In *tra-2(e1095); mpk-1* RNAi XX testis, we observe feminization based on high *rme-2* mRNA accumulation as well as pachytene arrest and pachytene cellular disorganization phenotypes (Figure 7, F and G; supplemental Table 5 at http://www.genetics.org/supplemental/). Germline feminization was observed with *tra-2(e1095); mpk-1(ga117)* XX mutants, although epistasis was incomplete as 11% of germlines displayed male development (supplemental Table 5). We have not observed feminization of somatic tissue either in *mpk-1* null XO males or in the *tra-2(e1095); mpk-1(ga117)* XX double mutant, which is a background that is more sensitive to partial feminization, suggesting that MPK-1 does not have an essential function in somatic sex determination. We conclude that MPK-1 acts downstream or in parallel with TRA-2 to promote the male germ cell fate. Epistasis analysis with *fem-3(q20gf)* is consistent with this interpretation; *fem-3(q20gf)* XX mutant hermaphrodites at 25° have a fully masculinized germline and a female soma (Barton *et al.* 1987) while the *mpk-1(ga117); fem-3(q20gf)* mutants at 25° have a feminized germline (data not shown).

MPK-1 ERK has the nonessential function of promoting the proliferative germ cell fate: At the distal end of the gonad, GLP-1 Notch signaling promotes the germline stem cell fate, producing a population of 200–230 mitotically cycling cells that extend ~20 cell diameters from the distal tip (Kimble and Crittenden 2006; Hansen and Schedl 2006). As proliferative germ cells are observed in null/strong lf mutants, LIN-45, MEK-2, and MPK-1 do not have an essential function in germ cell proliferation (Table 1; Figures 3D and 7C). However, there is a significant reduction in the number of proliferating germ cells in *mpk-1(ga117)* young adults (170 *vs.* 232 for wild type at 18 hr post L4) that further decreases with age (supplemental Table 6 at http://www.genetics.org/supplemental/). This reduction could be because LIN-45, MEK-2, and MPK-1 have a nonessential function to promote proliferation in the proliferation *vs.* meiotic development decision, have a nonessential function in mitotic cell cycle progression, or both. Mutations in *glp-1* provide sensitized backgrounds that can be used to identify genes that function in the control of the proliferation *vs.* meiotic development decision, even if the function is nonessential. Mutations (lf) that enhance the weak ts *glp-1* lf allele *bn18* at the permissive temperature, leading to all proliferative germ cells entering meiotic prophase, identify genes that promote the proliferative fate (Qiao *et al.* 1995), while germline autonomous lf mutations that enhance the weak *glp-1* gf allele *ar202*, leading to overproliferation/tumorous germlines, identify genes that promote meiotic development (Hansen *et al.* 2004).

We found that null mutations in *mpk-1* and *lin-45* and a strong lf *mek-2* allele enhance the premature meiotic entry defect of *glp-1(bn18)* at the permissive temperature (Figure 8; supplemental Table 7 at http://www.genetics.org/supplemental/). Thus MPK-1, MEK-2, and LIN-45 function to promote the proliferative fate; however, since the single mutants retain proliferative cells, this function must be nonessential. The observed premature meiotic entry (Glp) phenotype occurred late, in L4's or in young adults, possibly because of maternal rescue, and while highly penetrant, a low percentage of gonads retained a small number of proliferative germ cells. MPK-1 might function in the germline or the somatic gonad to promote proliferation. To distinguish between these possibilities, we compared enhancement of *glp-1(bn18)* following *mpk-1* RNAi in either an *rrf-1* null or a wild-type background. We found an equivalent frequency in wild-type and *rrf-1* null backgrounds (supplemental Table 7), indicating that MPK-1 functions in the germline to promote germline proliferation. We considered the possibility that the severe disruption in organization of meiotic prophase germ cells on the surface of the gonad tube in *lin-45*, *mek-2*, and *mpk-1* mutants might nonspecifically disrupt trafficking of germline regulators, leading to enhancement *of glp-1(bn18)*. However, the extent of disorganization of meiotic prophase cells was not correlated with premature meiotic entry; germlines that show premature meiotic entry can have mild disorganization of meiotic prophase cells while germlines that retained some proliferative germ cells can have strong disorganization of meiotic prophase cells.

Thompson *et al.* (2005) have shown that *fog-1*, *fog-3*, and *fem-3* genes that promote the male germ cell fate also have the nonessential function of promoting the proliferative fate. This was based on the finding that null mutations in these genes enhanced the premature meiotic entry phenotype of the *fbf-1 fbf-2* null double mutant (Crittenden *et al.* 2002). Since *mpk-1*, like *fog-1*, *fog-3*, and *fem-3*, promote the male germ cell fate, we asked if the enhancement of *glp-1(bn18)* by *mpk-1*, *mek-2*, and *lin-45* was a reflection of the LIN-45/MEK-2/MPK-1-signaling module acting at the same step as FOG-1/

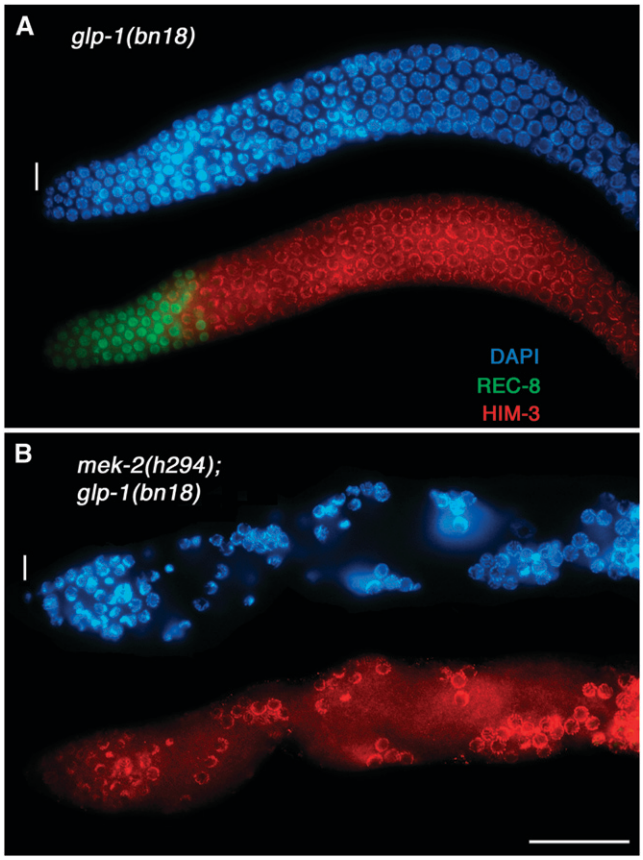

Figure 8.—MPK-1 has the nonessential function of promoting the proliferative germline fate. Adult *glp-1(bn18)* or *mek-2(h294); glp-1(bn18)* hermaphrodites 24 hr post L4 at 20° were dissected and stained for REC-8 (green), which, under our conditions, marks nuclei in the proliferation/mitotic zone (Hansen *et al.* 2004), and for HIM-3 (red), which marks nuclei in meiotic prophase germ cells and chromosome morphology (DAPI, blue). (A) In *glp-1(bn18)*, germ cells proliferate and enter meiotic prophase. (B) In *mek-2(h294); glp-1 (bn18)*, the proliferative population is lost and all germ cells have entered meiotic prophase on the basis of all nuclei staining positive for HIM-3 and staining negative for REC-8. Identical results are observed for *glp-1(bn18)* with *mpk-1(ga117)* or *lin-45(dx19)*.

FOG-3/FEM-3 in the proliferation *vs.* meiosis decision. Surprisingly, we found that *mpk-1* null did not enhance the premature meiotic entry phenotype of the *fbf-1 fbf-2* null double mutant, although it did feminize the germline, and that *fog-1* null did not enhance the premature meiotic entry defect of *glp-1(bn18)* (supplemental Table 7 at http://www.genetics.org/supplemental/; data not shown). Thus the nonessential function of MPK-1 of promoting the germline proliferative fate appears to be distinct from the nonessential function of FOG-1/FOG-3/FEM-3 of promoting the proliferative fate.

DISCUSSION

Work described here demonstrates that MPK-1 ERK is dynamically activated to control and coordinate multiple aspects of *C. elegans* germline development. From genetic analysis we infer eight distinct processes that are controlled by MPK-1 (Table 4). MPK-1 functions in four developmental switches: progression from distal to proximal pachytene, oocyte maturation/ovulation, specification of the male germ cell fate, and the nonessential function of promoting the proliferative germ cell fate. Importantly, MPK-1 also regulates multiple aspects of cell biology during oogenesis, including control of cellular morphogenesis and membrane organization. MPK-1 is required for the gonadal tube arrangement of pachytene cells on the surface and an interior cytoplasmic rachis (pachytene cellular organization), forming a single row of cylindrically shaped oocytes in the proximal gonad (oocyte organization and differentiation), oocyte growth control, and migration of the oocyte nucleus to the distal surface. Genetic analysis as well as the pattern of activation indicates that these MPK-1 functions are largely or completely germline autonomous (Table 4). The eight processes are cell biologically diverse and it is likely that MPK-1 directs the different processes, in part, through phosphorylating distinct substrates or sets of substrates. The assembly line production of oocytes in the worm germline requires exquisite temporal and spatial coordination of many events, including morphogenetic processes, biosynthesis and packaging of materials, and meiotic chromosome changes of pachytene progression and maturation/ovulation of the -1 oocyte. Of processes that are controlled by MPK-1, some are contemporaneous (*e.g.*, pachytene progression and pachytene cellular organization) while others are sequential (*e.g.*, pachytene cellular organization and oocyte organization and differentiation). Thus, MPK-1 likely functions not only in the execution of individual processes but also in the coordination and integration of contemporaneous and sequential processes.

It is possible that MPK-1 has additional functions in germline development that are not revealed by experiments reported here. We used (1) ts *mpk-1* lf mutants and partial *mpk-1* RNAi to uncover phenotypes, and thus functions, not observed in null mutants and (2) *let-60* gf mutants to examine effects of increased MPK-1 activity. However, gene functions are not equivalently affected under these conditions. For example, vulval development and hermaphrodite spermatogenesis are essentially normal in *mpk-1(ga111)* at 25°. The ability to detect partial lf phenotypes by RNAi depends on the kinetics of depletion as well as on the kinetics of germline development. These insensitivities may have led to a failure to produce phenotypic defects in certain processes. Furthermore, other aspects of germline development, such as microtubule organization during oogenesis (Harris *et al.* 2006), were not examined. Work reported here has focused on MPK-1 function although, for some of the processes, we show that LIN-45 RAF and MEK-2 MEK act with MPK-1 as part of the

TABLE 4

Summary of MPK-1 germline functions, associated phenotypes, and site of action

	MPK-1 germline functions							
	Pachytene progression	Pachytene cellular organization	Oocyte organization and differentiation	Oocyte growth control	Oocyte nuclear migration	Oocyte maturation and ovulation	Specification of male fate[a]	Promotion of proliferative fate (nonessential)
mpk-1 lf phenotype	Nuclei arrested in pachytene	Gaps or absence of cells on the surface of the gonad, loss of rachis	Disorganized shape/position of oocytes, multinucleate oocytes	Large oocytes	Centrally located oocyte nucleus	Delayed or failed maturation and ovulation; Emo	Feminized hermaphrodite and male germlines	Enhancement of *glp-1(bn18)* premature meiotic entry
Site of *mpk-1* function	Germline[b]	Germline[b]	Germline[c]	Germline[c]	Germline[c]	Likely germline[d]	Germline[c]	Germline[c]
Pathway genes known to be involved in process	*let-60*, *ksr-2*, *lin-45*, *mek-2*	*let-60*, *ksr-2*, *lin-45*, *mek-2*	—	*let-60*, *ptp-2*	—	—	*lin-45*, *mek-2*	*lin-45*, *mek-2*

[a] It is not currently known if *let-60* and *ksr-2* function in male germline sex determination. For the *let-60(dx16)* allele, which is a genetic and molecularly null (see supplemental Table 8 and legend at http://www.genetics.org/supplemental/), adult hermaphrodite escapers of L1 lethality make sperm followed by pachytene-arrested cells, suggesting that *let-60* does not function in promoting the male germ cell fate. However, as a number of germline sex determination genes show maternal effects (*e.g.*, Doniach and Hodgkin 1984), we cannot rule out the possibility that the male germ cells produced in *let-60(dx16)* homozygotes are a consequence of maternally supplied *let-60(+)*. Similarly, *ksr-2* null mutant hermaphrodites make sperm (Ohmachi *et al.* 2002), which could also be a result of maternal rescue. Male germ cell fate specification in *let-60* and *ksr-2* null XO male mutants has not yet been examined.

[b] Mosaic analysis from Church *et al.* (1995) and RNAi in *rrf-1(pk1417)* null (supplemental Table 1 at http://www.genetics.org/supplemental/).

[c] RNAi in *rrf-1* null (supplemental Tables 1, 4, 5, and 7).

[d] Based on (1) Emo phenotype following RNAi in *rrf-1* null and (2) strong dpMPK-1 staining in proximal oocytes in hermaphrodites but not in females. However, since time-lapse video analysis has not been performed to determine the basis of the Emo phenotype and because dpMPK-1 is detected in sheath cell nuclei, we cannot rule out that MPK-1 may also function in sheath cells to promote maturation/ovulation.

TABLE 5

Position and duration of MPK-1 activation (dpMPK-1) in *C. elegans* germline development

	Hermaphrodite[a]			Young adult female[b]	Male[c]
Position/stage	Proximal pachytene (peak)	Diplotene/early diakinesis (valley)	-1 through -5 oocytes (peak)	Newly formed diakinesis oocyte (peak)	Proximal transition zone/distal pachytene (peak)
Duration	~18 hr (sustained)	~160 min (sustained)	~110 min (sustained)	~30 min (transient)	~6 hr (sustained)

Duration estimated from the length in cell diameters displaying dpMPK-1 above background relative to the time required for a germ cell to transit through the relevant region of the germline as determined by Cy3-dUTP pulse-chase studies or time-lapse video analysis (McCarter *et al.* 1999; Jaramillo-Lambert *et al.* 2007).

[a] Hermaphrodite ~24 hr post L4.

[b] Young adult female 6–8 hr post L4.

[c] Male ~24 hr post L4.

canonical cascade (Table 4). However, further studies will be necessary to more fully define the cascade members upstream of MPK-1 that function in the different processes.

Activation of MPK-1 in the germline is temporally/spatially dynamic compared with relatively modest changes in total MPK-1 (Figures 1, 2, and 3; Table 3; supplemental Figure 2 at http://www.genetics.org/supplemental/; Miller *et al.* 2001; Page *et al.* 2001). Active MPK-1 is present in both the cytoplasm and the nucleus, consistent with functions in membrane/cytoplasmic morphogenetic events, meiotic chromosome dynamics, and probable changes in transcription (Table 4; Leacock and Reinke 2006). In mammalian systems, ERK activation has been classified as either transient (≤30 min) or sustained (≥1 hr), with both observed *in vivo* in cell-type-specific patterns that are likely important for normal embryogenesis and organogenesis (Marshall 1995; Corson *et al.* 2003; Fata *et al.* 2007). Previous studies have determined the time that it takes for a germ cell to transit proximally through a given stage of meiotic prophase/gametogenesis (McCarter *et al.* 1999; Jaramillo-Lambert *et al.* 2007). Combining the transit time and the number of cell diameters in length that a particular region shows dpMPK-1 accumulation, we can estimate the duration of MPK-1 activation. The dpMPK-1 observed in hermaphrodites and males corresponds to sustained MPK-1 activation in the various regions (Table 5); for example, a germ cell will be dpMPK-1 positive for ~18 hr as it moves through the 18 cell diameters in length of proximal pachytene. By contrast, the dpMPK-1 detected in the newly formed diakinesis oocyte of young adult females corresponds to transient activation. In some cases, a germline process can be attributed to a specific spatial region of MPK-1 activation (pachytene progression is likely mediated by MPK-1 activation in pachytene), but in other cases the causal region of MPK-1 activation is less clear (male sex determination; see below). While our ability to detect dpMPK-1 is reproducible and appears sensitive, it remains possible that we have failed to detect active MPK-1 in certain regions of the germline. This possibility is suggested by our finding that MPK-1 acts germline autonomously to promote the proliferative germ cell fate (Table 4) although we fail to detect dpMPK-1 in the distal germline.

MPK-1 activation is important for a number of germline processes; however, there is not a simple relationship between dpMPK-1 level and normal development. *mpk-1(ga111)* contains a missense mutation near the activation loop and thus may have a temperature-dependent defect in activation by MEK-2 (Lackner and Kim 1998). *mpk-1(ga111)* hermaphrodites at 20° have low but detectable levels of dpMPK-1 (supplemental Figure 12 at http://www.genetics.org/supplemental/), yet animals are fertile and for the most part the germline is normal, with maturations/ovulations occurring ~2.7-fold slower than in wild type. Conversely, in *let-60(ga89gf)* hermaphrodites at 20°, dpMPK-1 levels rise prematurely in pachytene and are elevated in diplotene and diakinesis (Figures 2 and 3; supplemental Figures 4 and 8), yet animals are fertile and the germline for the most part is normal, with germ cells apparently progressing through pachytene prematurely. Thus, within these limits, obvious cytological differences in dpMPK-1 level are tolerated with respect to fertility, although these germlines are clearly sensitized to further changes in gene activity following shift to the restrictive temperature.

What are the signaling pathways that generate the dynamic pattern of MPK-1 activation? Sperm-derived MSP signaling through the VAB-1 Ephrin (Eph) receptor in oocytes and additional receptors in oocytes and somatic gonadal sheath cells leads to MPK-1 activation in the -1 to -5 oocytes (see below; Miller *et al.* 2001, 2003; Corrigan *et al.* 2005; Govindan *et al.* 2006). LET-23 EGF-like receptor signaling through MPK-1 is important for a number of cell fate decisions in the worm (Moghal and Sternberg 2003). While *let-23* is required for fertility, MPK-1 activation occurs normally in *let-23* mutants, and *let-23* functions in the somatic

gonad, not the germline, to promote oocyte ovulation (J. McCarter, M.-H. Lee and T. Schedl, unpublished observations). Thus much remains to be learned about the upstream receptors and the downstream gene products that generate the dynamic pattern.

MPK-1 function and activation in pachytene: Reduction or elimination of *mpk-1* activity results in germ cells arrested in pachytene and loss of both the gonadal tube arrangement of pachytene cells on the surface and the interior cytoplasmic rachis (Table 4). In our analysis we did not identify a condition where pachytene arrest and pachytene cellular disorganization were separately disrupted, leading to the possibility that they represent a single pachytene function. However, in recent work in identifying phosphorylation substrates of MPK-1, we have separated the functions by discovering substrates that display only one or the other mutant phenotype, thus indicating that MPK-1 has at least two pachytene functions: one controlling pachytene progression and the other controlling pachytene cellular organization (S. Arur, M. Ohmachi, S. Nayak and T. Schedl, unpublished observations).

In pachytene, sustained MPK-1 activation is observed in surface pachytene germ cells (nuclei and cytoplasm) and in the interior rachis. The rise in activated MPK-1 almost midway through pachytene appears to promote a switch of germ cells from distal to proximal pachytene. This view is supported by markers demonstrating that *mpk-1(ga117)* null germ cells arrest with mid-pachytene characteristics, high DAZ-1, absence of CEP-1/high GLD-1, and nuclei displaying a symmetric/dispersed pachytene organization (Figure 3; supplemental Figure 3 at http://www.genetics.org/supplemental/). Furthermore, in *let-60(ga89gf)*, the earlier rise in dpMPK-1 level compared to wild type appears to lead to a premature transition from distal to proximal pachytene as judged by the premature fall in DAZ-1 levels and a shortening in the total length of pachytene.

It is not known which activities are controlled by MPK-1 for the switch from distal to proximal pachytene. Although the *mpk-1* null pachytene-arrest phenotype suggests an essential function in meiotic recombination/chromosome dynamics (Roeder and Bailis 2000), two lines of reasoning indicate a broader role. First, currently known single-gene mutations that disrupt meiotic chromosome pairing, synapsis, double-strand break formation, and recombination do not arrest meiotic prophase progression and do not prevent formation of oocytes (*e.g.*, Dernburg *et al.* 1998; MacQueen and Villeneuve 2001; Rinaldo *et al.* 2002; Colaiacovo *et al.* 2003). Second, changes in *mpk-1* activity alter the spatial pattern of the cytoplasmic proteins DAZ-1 and GLD-1, indicating effects outside meiotic recombination/chromosome dynamics. Thus a number of MPK-1 substrates and effectors are likely involved in coordinating progression from distal to proximal pachytene.

MPK-1 function in pachytene cellular organization involves control of membrane and cytoskeletal organization in the pachytene region. Thus, while progression from distal to proximal pachytene might require only transient MPK-1 activation, it is likely that pachytene cellular organization requires continuous function and therefore sustained activation. Other activities that occur in proximal pachytene that may be directly or indirectly controlled by MPK-1 may also require sustained activation. These include germ cell apoptosis (Gumienny *et al.* 1999; Kritikou *et al.* 2006; S. Arur, C. Schertel, B. Conradt and T. Schedl, unpublished observations), cytoplasmic streaming, and changes in transcription and translation that are important for later aspects of oogenesis in the proximal germline (Lee and Schedl 2001; Kelly *et al.* 2002; Leacock and Reinke 2006; Wolke *et al.* 2007). Thus, MPK-1 activation in pachytene may coordinate diverse processes in pachytene as well as integrate pachytene processes with later oogenesis.

MPK-1 acts as a rheostat in oocyte growth control: Oocytes are unique cells in animals that can achieve sizes >1000 times that of diploid somatic cells. Large oocytes are generated under conditions where MPK-1 activity is reduced, employing *mpk-1(ga111)* shift-ups, partial *mpk-1* RNAi, *let-60(n1046dx1)*, or *ptp-2* null (Figure 5B; Church *et al.* 1995; Gutch *et al.* 1998). Conversely, small oocytes are generated under a condition where MPK-1 activity is increased: *let-60(ga89gf)* shift-up (Figure 5C; supplemental Figure 11 at http://www.genetics.org/supplemental/). Thus, MPK-1 appears to act as a rheostat to control oocyte size, with low MPK-1 activity promoting growth, high MPK-1 activity inhibiting growth, and, presumably, normal-size oocytes produced at intermediate MPK-1 activity. Activated MPK-1 in diplotene and diakinesis appears to be involved in oocyte growth control, although it is possible that pachytene MPK-1 activity also contributes. Recent work by Wolke *et al.* (2007) has shown that oocyte growth is, in part, accomplished by actin-filament-mediated cytoplasmic streaming of material from the rachis into the oocyte through cytoplasmic bridges. MPK-1 could modulate cytoplasmic streaming at any one of a number of steps to control oocyte growth.

MPK-1 is required for timely oocyte meiotic maturation and ovulation: In vertebrates, ERK activation functions in promoting events of oocyte meiotic maturation and/or the transition to and maintenance of meiosis II arrest (Fan and Sun 2004; Liang *et al.* 2007). In *C. elegans*, MPK-1 activation and oocyte maturation/ovulation are MSP/sperm dependent (McCarter *et al.* 1999; Miller *et al.* 2001; Page *et al.* 2001), but it was not known if MPK-1 function was required for the process. Here we show that MPK-1, at a minimum, is required for timely oocyte maturation/ovulation and may be required to initiate the transition. This view is supported by the observation that the point of delay/arrest when

MPK-1 activity is reduced following *mpk-1(ga111)* shift-up is the same as the arrest point in females.

The MSP/sperm-dependent strong MPK-1 activation in the most proximal approximately five oocytes is likely responsible for MPK-1's function in maturation/ovulation (Figures 2 and 4; supplemental Figures 7 and 8 at http://www.genetics.org/supplemental/). However, in the germline assembly line only the -1 oocyte undergoes maturation. MPK-1 activation thus is not sufficient and additional regulatory mechanisms, such as inhibition of CDK-1 from proximal oocytes and/or inhibition from somatic gonadal sheath cells, must block maturation of the -2 through -5 oocytes (McCarter *et al.* 1999; Burrows *et al.* 2006; Govindan *et al.* 2006). We observe that levels of activated MPK-1 vary considerably in the -2 through -5 oocytes, even within the same gonad; the significance of this variability is unclear and the mechanism by which the variability is generated is not known.

Activated MPK-1 falls dramatically as the -1 oocyte undergoes maturation, even in *let-60(ga89gf)* mutants where dpMPK-1 levels are significantly elevated in proximal oocytes (Figures 1, 2, and 4; supplemental Figure 8 at http://www.genetics.org/supplemental/; Page *et al.* 2001). This inactivation of MPK-1 is distinct from the pattern in vertebrates where active ERK is present from maturation until release of the meiosis II arrest by fertilization. The difference likely reflects differences in reproductive biology. In vertebrates, the meiosis II arrest is maintained by active ERK and thereby allows fertilization to be temporally/spatially separate from maturation, meiosis I, and ovulation. In *C. elegans*, the events of maturation, ovulation into the spermatheca, fertilization, and completion of the meiotic divisions occur in rapid succession and a meiosis II arrest is not necessary since maturation/ovulation does not occur unless sperm are available for immediate fertilization. The abrupt fall in dpMPK-1 levels during maturation may ensure that active MPK-1 does not lead to delay or arrest of meiosis II. Additionally, it has been proposed that active ERK inhibits sperm centrosome function in a variety of vertebrates and invertebrates (Stephano and Gould 2000). In *C. elegans*, the sperm centrosome may trigger the completion of female meiosis and appears to function in anterior/posterior axis formation at the one-cell stage (Sadler and Shakes 2000; Wallenfang and Seydoux 2000; Cowan and Hyman 2004; McNally and McNally 2005). The removal of active MPK-1 during maturation may be important to ensure that subsequent processes mediated by the sperm centrosome are not inhibited.

The effects of MSP/sperm signaling on MPK-1 activation and function: From analysis of dpMPK-1 levels in wild-type and female backgrounds, we propose that MSP/sperm signaling has at least three major effects. First, as previously described, MSP/sperm signaling through the VAB-1 Eph receptor and other receptors leads to MPK-1 activation in the -1 through -5 oocytes to promote maturation/ovulation (see above; Miller *et al.* 2001, 2003). Second, MSP/sperm signaling leads to MPK-1 activation in diplotene and diakinesis that likely functions in oocyte growth control (see above). Third, MSP/sperm signaling by promoting maturation/ovulation leads to flux in the germline assembly line that results in MPK-1 activation that is MSP/sperm independent. This proposal is based on differences in MPK-1 activation between young adult females that generate new oocytes and older adult females that do not. In young females where new oocytes are being generated, cytoplasmic streaming occurs, and germ cells progress through pachytene, we found active MPK-1 in pachytene (Figure 2; supplemental Figure 9 at http://www.genetics.org/supplemental/; Wolke *et al.* 2007). Young adult females also have transiently activated MPK-1 in a single diakinesis oocyte, usually the second oocyte proximal to the last diplotene oocyte; the function of this activation is not currently known. By contrast, in older adult females with >15 diakinesis oocytes, where new oocytes are not being generated, cytoplasmic streaming does not occur and germ cells progress through pachytene at a slow rate (Jaramillo-Lambert *et al.* 2007; Wolke *et al.* 2007), we observe very low levels of activated MPK-1 in pachytene, diplotene, and diakinesis (Figure 2, supplemental Figure 9). The MPK-1 activation in young adult females is, by definition, MSP/sperm independent and occurs when flux through the germline is generating new oocytes, unlike in older adult females. MSP/sperm thus can lead to MPK-1 activation in two ways: directly by binding to receptors such as VAB-1 and indirectly by inducing maturation/ovulation that leads to distal flux through the germline assembly line. How flux of germ cells through the oocyte assembly line leads to MSP/sperm-independent MPK-1 activation is unknown.

MPK-1 is necessary for the male germ cell fate: Germline sex determination genes necessary for the male fate have been identified on the basis of lf phenotype of germ cells that would normally form sperm but instead form oocytes (Doniach and Hodgkin 1984; Kimble *et al.* 1984). A role for MPK-1 in germline sex determination was not previously recognized since strong lf mutations show pachytene arrest and cellular disorganization that preclude the formation of sperm or oocytes. We used sexually dimorphic markers that are expressed prior to overt gametogenesis to assess the sexual identity of the pachytene-arrested and disorganized germ cells. We found that MPK-1 is required for the male germ cell fate in both hermaphrodites and males. This MPK-1 function is germline autonomous and appears to be required continuously, at least in males.

In the *C. elegans* germline sex determination pathway, the *tra-2* gene promotes the female fate by repressing the downstream *fem-1*, *-2*, and *-3* and *fog-1* and *-3* genes, which act near the end of the cascade to specify the male fate. Our genetic epistasis analysis indicates that male

development in the *tra-2* null mutant depends on *mpk-1* activity, indicating that MPK-1 acts either downstream of TRA-2 (with the FEMs and FOGs) or in a parallel pathway. The epistasis is not complete (~11% of germlines show some male development), suggesting that another gene(s) acts redundantly with MPK-1, although with a lesser role. Support for the possibility that MPK-1 acts in parallel or separately from the FEMs and FOG-1 and FOG-3 comes from our finding that the nonessential function of MPK-1 in promoting the proliferative fate is genetically distinct from the nonessential function of FOG-1, FOG-3, and FEM-3 in promoting the proliferative fate.

Sustained MPK-1 activation is observed from the proximal transition zone through early pachytene in the male gonad while dpMPK-1 staining is not observed in this region in adult hermaphrodites (Figures 1 and 7A; Table 5). This active MPK-1 may be responsible for specification of the male fate. However, sexually dimorphic FOG-1 expression occurs distal or earlier than dpMPK-1 accumulation; Thompson *et al.* (2005) found low but detectable levels of FOG-1 in the proximal half of the mitotic region with higher levels in the distal transition zone through pachytene in adult males while adult hermaphrodites, which have long completed spermatogenesis, lack FOG-1. One possibility for the spatially distinct patterns in the male germline is that MPK-1 function in specification of the male fate is in parallel, although somewhat temporally delayed, to the pathway that controls FOG-1 levels. Alternatively, the MPK-1 activity responsible for the male germ cell fate occurs earlier in the proximal mitotic region/distal transition zone but is below the limit of dpMPK-1 detection. Additionally, it is possible that the dpMPK-1 observed in the proximal transition zone through early pachytene represents activation for an MPK-1 function in male meiotic prophase and/or spermatogenesis that is masked by the germline feminization.

Perspectives: The dynamic pattern of MPK-1 activation and the identification of eight germline processes controlled by MPK-1 lead to a number of questions relevant to both *C. elegans* germline development and MPK-1 signaling. What are the upstream signals that lead to MPK-1 control of a specific germline process(es)? For example, is there a systemic signal that promotes male germline sex determination in both the hermaphrodite and male that leads to MPK-1 activation? What are the upstream signaling pathways and feedback loops that generate specific patterns of sustained or transient MPK-1 activation? What are the downstream MPK-1 substrates that execute a given germline process(es)? How is MPK-1 activation and substrate phosphorylation spatially controlled so that specific germline processes are executed and coordinated? Given the conservation of ERK signaling in animals, information obtained in *C. elegans* is likely to be relevant to ERK function in other systems.

We acknowledge Andrew Godbey for help in the initial stages of this work. We thank our many colleagues for helpful discussions throughout the course of the study. We thank Dave Hansen, Associate Editor, and the reviewers for constructive and insightful comments on the manuscript. We are grateful to our colleagues Michael Gloltzer, David Greenstein, Patty Kuwabara, Verena Jantsch-Plunger, Josef Loidl, Jill Schumacher, Masayuki Yammamoto, and Monique Zetka for antibodies. Some of the strains used in this study were supplied by the *Caenorhabditis* Genetics Center. Work in the Schedl laboratory was funded by National Institutes of Health grant GM63310.

LITERATURE CITED

Barton, M. K., T. B. Schedl and J. Kimble, 1987 Gain-of-function mutations of *fem-3*, a sex-determination gene in *Caenorhabditis elegans*. Genetics **115:** 107–119.

Beitel, G. J., S. G. Clark and H. R. Horvitz, 1990 Caenorhabditis elegans ras gene let-60 acts as a switch in the pathway of vulval induction. Nature **348:** 503–509.

Burrows, A. E., B. K. Sceurman, M. E. Kosinski, C. T. Richie, P. L. Sadler *et al.*, 2006 The C. elegans Myt1 ortholog is required for the proper timing of oocyte maturation. Development **133:** 697–709.

Carlton, P. M., A. P. Farruggio and A. F. Dernburg, 2006 A link between meiotic prophase progression and crossover control. PLoS Genet. **2:** e12.

Chin, G. M., and A. M. Villeneuve, 2001 C. elegans mre-11 is required for meiotic recombination and DNA repair but is dispensable for the meiotic G(2) DNA damage checkpoint. Genes Dev. **15:** 522–534.

Church, D. L., K. L. Guan and E. J. Lambie, 1995 Three genes of the MAP kinase cascade, mek-2, mpk-1/sur-1 and let-60 ras, are required for meiotic cell cycle progression in Caenorhabditis elegans. Development **121:** 2525–2535.

Colaiacovo, M. P., A. J. MacQueen, E. Martinez-Perez, K. McDonald, A. Adamo *et al.*, 2003 Synaptonemal complex assembly in C. elegans is dispensable for loading strand-exchange proteins but critical for proper completion of recombination. Dev. Cell **5:** 463–474.

Corrigan, C., R. Subramanian and M. A. Miller, 2005 Eph and NMDA receptors control Ca2+/calmodulin-dependent protein kinase II activation during C. elegans oocyte meiotic maturation. Development **132:** 5225–5237.

Corson, L. B., Y. Yamanaka, K. M. Lai and J. Rossant, 2003 Spatial and temporal patterns of ERK signaling during mouse embryogenesis. Development **130:** 4527–4537.

Cowan, C. R., and A. A. Hyman, 2004 Centrosomes direct cell polarity independently of microtubule assembly in C. elegans embryos. Nature **431:** 92–96.

Crittenden, S. L., D. S. Bernstein, J. L. Bachorik, B. E. Thompson, M. Gallegos *et al.*, 2002 A conserved RNA-binding protein controls germline stem cells in Caenorhabditis elegans. Nature **417:** 660–663.

Dernburg, A. F., K. McDonald, G. Moulder, R. Barstead, M. Dresser *et al.*, 1998 Meiotic recombination in C. elegans initiates by a conserved mechanism and is dispensable for homologous chromosome synapsis. Cell **94:** 387–398.

Doniach, T., and J. Hodgkin, 1984 A sex-determining gene, fem-1, required for both male and hermaphrodite development in Caenorhabditis elegans. Dev. Biol. **106:** 223–235.

Eisenmann, D. M., and S. K. Kim, 1997 Mechanism of activation of the *Caenorhabditis elegans* ras homologue let-60 by a novel, temperature-sensitive, gain-of-function mutation. Genetics **146:** 553–565.

Ellis, R., and T. Schedl, 2006 Sex determination in the germ line, in *Worm Book*, edited by The *C. elegans* Research Community. (http://www.wormbook.org).

Fan, H. Y., and Q. Y. Sun, 2004 Involvement of mitogen-activated protein kinase cascade during oocyte maturation and fertilization in mammals. Biol. Reprod. **70:** 535–547.

Fata, J. E., H. Mori, A. J. Ewald, H. Zhang, E. Yao *et al.*, 2007 The MAPK(ERK-1,2) pathway integrates distinct and antagonistic signals from TGFalpha and FGF7 in morphogenesis of mouse mammary epithelium. Dev. Biol. **306:** 193–207.

Francis, R., M. K. Barton, J. Kimble and T. Schedl, 1995 gld-1, a tumor suppressor gene required for oocyte development in *Caenorhabditis elegans*. Genetics **139:** 579–606.

Gartner, A., S. Milstein, S. Ahmed, J. Hodgkin and M. O. Hengartner, 2000 A conserved checkpoint pathway mediates DNA damage-induced apoptosis and cell cycle arrest in C. elegans. Mol. Cell **5:** 435–443.

Gibert, M. A., J. Starck and B. Beguet, 1984 Role of the gonad cytoplasmic core during oogenesis of the nematode Caenorhabditis elegans. Biol. Cell **50:** 77–85.

Govindan, J. A., H. Cheng, J. E. Harris and D. Greenstein, 2006 Galphao/i and Galphas signaling function in parallel with the MSP/Eph receptor to control meiotic diapause in C. elegans. Curr. Biol. **16:** 1257–1268.

Grant, B., and D. Hirsh, 1999 Receptor-mediated endocytosis in the Caenorhabditis elegans oocyte. Mol. Biol. Cell **10:** 4311–4326.

Gumienny, T. L., E. Lambie, E. Hartwieg, H. R. Horvitz and M. O. Hengartner, 1999 Genetic control of programmed cell death in the Caenorhabditis elegans hermaphrodite germline. Development **126:** 1011–1022.

Gutch, M. J., A. J. Flint, J. Keller, N. K. Tonks and M. O. Hengartner, 1998 The Caenorhabditis elegans SH2 domain-containing protein tyrosine phosphatase PTP-2 participates in signal transduction during oogenesis and vulval development. Genes Dev. **12:** 571–585.

Hall, D. H., V. P. Winfrey, G. Blaeuer, L. H. Hoffman, T. Furuta *et al.*, 1999 Ultrastructural features of the adult hermaphrodite gonad of Caenorhabditis elegans: relations between the germ line and soma. Dev. Biol. **212:** 101–123.

Han, M., R. V. Aroian and P. W. Sternberg, 1990 The *let-60* locus controls the switch between vulval and nonvulval cell fates in *Caenorhabditis elegans*. Genetics **126:** 899–913.

Hansen, D., and T. Schedl, 2006 The regulatory network controlling the proliferation-meiotic entry decision in the Caenorhabditis elegans germ line. Curr. Top. Dev. Biol. **76:** 185–215.

Hansen, D., E. J. Hubbard and T. Schedl, 2004 Multi-pathway control of the proliferation versus meiotic development decision in the Caenorhabditis elegans germline. Dev. Biol. **268:** 342–357.

Harris, J. E., J. A. Govindan, I. Yamamoto, J. Schwartz, I. Kaverina *et al.*, 2006 Major sperm protein signaling promotes oocyte microtubule reorganization prior to fertilization in Caenorhabditis elegans. Dev. Biol. **299:** 105–121.

Hirsh, D., D. Oppenheim and M. Klass, 1976 Development of the reproductive system of Caenorhabditis elegans. Dev. Biol. **49:** 200–219.

Hodgkin, J., 1980 More sex-determination mutants of *Caenorhabditis elegans*. Genetics **96:** 649–664.

Hodgkin, J., and T. Doniach, 1997 Natural variation and copulatory plug formation in *Caenorhabditis elegans*. Genetics **146:** 149–164.

Hsu, V., C. L. Zobel, E. J. Lambie, T. Schedl and K. Kornfeld, 2002 *Caenorhabditis elegans* lin-45 raf is essential for larval viability, fertility and the induction of vulval cell fates. Genetics **160:** 481–492.

Huang, P., and M. J. Stern, 2004 FGF signaling functions in the hypodermis to regulate fluid balance in C. elegans. Development **131:** 2595–2604.

Hubbard, E. J., and D. Greenstein, 2000 The Caenorhabditis elegans gonad: a test tube for cell and developmental biology. Dev. Dyn. **218:** 2–22.

Iwasaki, K., J. McCarter, R. Francis and T. Schedl, 1996 emo-1, a Caenorhabditis elegans Sec61p gamma homologue, is required for oocyte development and ovulation. J. Cell Biol. **134:** 699–714.

Jantsch-Plunger, V., and M. Glotzer, 1999 Depletion of syntaxins in the early Caenorhabditis elegans embryo reveals a role for membrane fusion events in cytokinesis. Curr. Biol. **9:** 738–745.

Jaramillo-Lambert, A., M. Ellefson, A. M. Villeneuve and J. Engebrecht, 2007 Differential timing of S phases, X chromosome replication, and meiotic prophase in the C. elegans germ line. Dev. Biol. **308:** 206–221.

Jones, A. R., R. Francis and T. Schedl, 1996 GLD-1, a cytoplasmic protein essential for oocyte differentiation, shows stage- and sex-specific expression during Caenorhabditis elegans germline development. Dev. Biol. **180:** 165–183.

Kelly, W. G., C. E. Schaner, A. F. Dernburg, M. H. Lee, S. K. Kim *et al.*, 2002 X-chromosome silencing in the germline of C. elegans. Development **129:** 479–492.

Kimble, J., and S. L. Crittenden, 2006 Germline proliferation and its control, in *Worm Book*, edited by The *C. elegans* Research Community. (http://www.wormbook.org).

Kimble, J., L. Edgar and D. Hirsh, 1984 Specification of male development in Caenorhabditis elegans: the fem genes. Dev. Biol. **105:** 234–239.

Kosinski, M., K. McDonald, J. Schwartz, I. Yamamoto and D. Greenstein, 2005 C. elegans sperm bud vesicles to deliver a meiotic maturation signal to distant oocytes. Development **132:** 3357–3369.

Kritikou, E. A., S. Milstein, P. O. Vidalain, G. Lettre, E. Bogan *et al.*, 2006 C. elegans GLA-3 is a novel component of the MAP kinase MPK-1 signaling pathway required for germ cell survival. Genes Dev. **20:** 2279–2292.

Kuwabara, P. E., M. H. Lee, T. Schedl and G. S. Jefferis, 2000 A C. elegans patched gene, ptc-1, functions in germ-line cytokinesis. Genes Dev. **14:** 1933–1944.

Lackner, M. R., and S. K. Kim, 1998 Genetic analysis of the *Caenorhabditis elegans* MAP kinase gene *mpk-1*. Genetics **150:** 103–117.

Lackner, M. R., K. Kornfeld, L. M. Miller, H. R. Horvitz and S. K. Kim, 1994 A MAP kinase homolog, mpk-1, is involved in ras-mediated induction of vulval cell fates in Caenorhabditis elegans. Genes Dev. **8:** 160–173.

Leacock, S. W., and V. Reinke, 2006 Expression profiling of MAP kinase-mediated meiotic progression in Caenorhabditis elegans. PLoS Genet. **2:** e174.

Lee, M. H., and T. Schedl, 2001 Identification of in vivo mRNA targets of GLD-1, a maxi-KH motif containing protein required for C. elegans germ cell development. Genes Dev. **15:** 2408–2420.

Lee, M. H., and T. Schedl, 2004 Translation repression by GLD-1 protects its mRNA targets from nonsense-mediated mRNA decay in C. elegans. Genes Dev. **18:** 1047–1059.

Liang, C. G., Y. Q. Su, H. Y. Fan, H. Schatten and Q. Y. Sun, 2007 Mechanisms regulating oocyte meiotic resumption: roles of mitogen-activated protein kinase. Mol. Endocrinol. **21:** 2037–2055.

MacQueen, A. J., and A. M. Villeneuve, 2001 Nuclear reorganization and homologous chromosome pairing during meiotic prophase require C. elegans chk-2. Genes Dev. **15:** 1674–1687.

Maddox, A. S., B. Habermann, A. Desai and K. Oegema, 2005 Distinct roles for two C. elegans anillins in the gonad and early embryo. Development **132:** 2837–2848.

Marshall, C. J., 1995 Specificity of receptor tyrosine kinase signaling: transient versus sustained extracellular signal-regulated kinase activation. Cell **80:** 179–185.

Maruyama, R., S. Endo, A. Sugimoto and M. Yamamoto, 2005 Caenorhabditis elegans DAZ-1 is expressed in proliferating germ cells and directs proper nuclear organization and cytoplasmic core formation during oogenesis. Dev. Biol. **277:** 142–154.

McCarter, J., B. Bartlett, T. Dang and T. Schedl, 1997 Soma-germ cell interactions in Caenorhabditis elegans: multiple events of hermaphrodite germline development require the somatic sheath and spermathecal lineages. Dev. Biol. **181:** 121–143.

McCarter, J., B. Bartlett, T. Dang and T. Schedl, 1999 On the control of oocyte meiotic maturation and ovulation in Caenorhabditis elegans. Dev. Biol. **205:** 111–128.

McNally, K. L., and F. J. McNally, 2005 Fertilization initiates the transition from anaphase I to metaphase II during female meiosis in C. elegans. Dev. Biol. **282:** 218–230.

Miller, M. A., V. Q. Nguyen, M. H. Lee, M. Kosinski, T. Schedl *et al.*, 2001 A sperm cytoskeletal protein that signals oocyte meiotic maturation and ovulation. Science **291:** 2144–2147.

Miller, M. A., P. J. Ruest, M. Kosinski, S. K. Hanks and D. Greenstein, 2003 An Eph receptor sperm-sensing control mechanism for oocyte meiotic maturation in Caenorhabditis elegans. Genes Dev. **17:** 187–200.

Moghal, N., and P. W. Sternberg, 2003 The epidermal growth factor system in Caenorhabditis elegans. Exp. Cell Res. **284:** 150–159.

Ohmachi, M., C. E. Rocheleau, D. Church, E. Lambie, T. Schedl *et al.*, 2002 C. elegans ksr-1 and ksr-2 have both unique and redundant functions and are required for MPK-1 ERK phosphorylation. Curr. Biol. **12:** 427–433.

Page, B. D., S. Guedes, D. Waring and J. R. Priess, 2001 The C. elegans E2F- and DP-related proteins are required for embryonic asymmetry and negatively regulate Ras/MAPK signaling. Mol. Cell **7:** 451–460.

Qiao, L., J. L. Lissemore, P. Shu, A. Smardon, M. B. Gelber *et al.*, 1995 Enhancers of *glp-1*, a gene required for cell-signaling in *Caenorhabditis elegans*, define a set of genes required for germline development. Genetics **141:** 551–569.

Rinaldo, C., P. Bazzicalupo, S. Ederle, M. Hilliard and A. La Volpe, 2002 Roles for *Caenorhabditis elegans rad-51* in meiosis and in resistance to ionizing radiation during development. Genetics **160:** 471–479.

Roeder, G. S., and J. M. Bailis, 2000 The pachytene checkpoint. Trends Genet. **16:** 395–403.

Rogers, E., J. D. Bishop, J. A. Waddle, J. M. Schumacher and R. Lin, 2002 The aurora kinase AIR-2 functions in the release of chromosome cohesion in Caenorhabditis elegans meiosis. J. Cell Biol. **157:** 219–229.

Rose, K. L., V. P. Winfrey, L. H. Hoffman, D. H. Hall, T. Furuta *et al.*, 1997 The POU gene ceh-18 promotes gonadal sheath cell differentiation and function required for meiotic maturation and ovulation in Caenorhabditis elegans. Dev. Biol. **192:** 59–77.

Rubin, G. M., H. C. Chang, F. Karim, T. Laverty, N. R. Michaud *et al.*, 1997 Signal transduction downstream from Ras in Drosophila. Cold Spring Harb. Symp. Quant. Biol. **62:** 347–352.

Sadler, P. L., and D. C. Shakes, 2000 Anucleate Caenorhabditis elegans sperm can crawl, fertilize oocytes and direct anterior-posterior polarization of the 1-cell embryo. Development **127:** 355–366.

Schlessinger, J., 2000 Cell signaling by receptor tyrosine kinases. Cell **103:** 211–225.

Schumacher, B., M. Hanazawa, M. H. Lee, S. Nayak, K. Volkmann *et al.*, 2005 Translational repression of C. elegans p53 by GLD-1 regulates DNA damage-induced apoptosis. Cell **120:** 357–368.

Schumacher, J. M., A. Golden and P. J. Donovan, 1998 AIR-2: an Aurora/Ipl1-related protein kinase associated with chromosomes and midbody microtubules is required for polar body extrusion and cytokinesis in Caenorhabditis elegans embryos. J. Cell Biol. **143:** 1635–1646.

Sijen, T., J. Fleenor, F. Simmer, K. L. Thijssen, S. Parrish *et al.*, 2001 On the role of RNA amplification in dsRNA-triggered gene silencing. Cell **107:** 465–476.

Stephano, J. L., and M. C. Gould, 2000 MAP kinase, a universal suppressor of sperm centrosomes during meiosis? Dev. Biol. **222:** 420–428.

Strome, S., 1986 Fluorescence visualization of the distribution of microfilaments in gonads and early embryos of the nematode Caenorhabditis elegans. J. Cell Biol. **103:** 2241–2252.

Sulston, J., and J. Hodgkin, 1988 Methods, pp. 587–606 in *The Nematode Caenorhabditis elegans*, edited by W. B. Wood. Cold Spring Harbor Laboratory Press, Cold Spring Harbor, NY.

Sundaram, M. V., 2006 RTK/Ras/MAPK signaling, in *Worm Book*, edited by The *C. elegans* Research Community. (http://www.wormbook.org).

Thompson, B. E., D. S. Bernstein, J. L. Bachorik, A. G. Petcherski, M. Wickens *et al.*, 2005 Dose-dependent control of proliferation and sperm specification by FOG-1/CPEB. Development **132:** 3471–3481.

Vojtek, A. B., and C. J. Der, 1998 Increasing complexity of the Ras signaling pathway. J. Biol. Chem. **273:** 19925–19928.

Wallenfang, M. R., and G. Seydoux, 2000 Polarization of the anterior-posterior axis of C. elegans is a microtubule-directed process. Nature **408:** 89–92.

Ward, S., and J. S. Carrel, 1979 Fertilization and sperm competition in the nematode Caenorhabditis elegans. Dev. Biol. **73:** 304–321.

Wolke, U., E. A. Jezuit and J. R. Priess, 2007 Actin-dependent cytoplasmic streaming in C. elegans oogenesis. Development **134:** 2227–2236.

Wu, Y., and M. Han, 1994 Suppression of activated Let-60 ras protein defines a role of Caenorhabditis elegans Sur-1 MAP kinase in vulval differentiation. Genes Dev. **8:** 147–159.

Yang, H. Y., K. McNally and F. J. McNally, 2003 MEI-1/katanin is required for translocation of the meiosis I spindle to the oocyte cortex in C elegans. Dev. Biol. **260:** 245–259.

Communicating editor: D. I. Greenstein